ECONOMISTS
FOR UKRAINE

WORKING PAPER SERIES

WORKING PAPER No. 13 NOVEMBER 2025

ESTIMATING THE ECONOMIC IMPACT OF THE RUSSIA-UKRAINE CONFLICT WITH NIGHTLIGHTS DATA

Luigi Buzzacchi, Antonio Matteo De Marco, and Francesco Luigi Milone

Economists for Ukraine (Econ4UA)

Website: https://econ4ua.org/ Email: info@econ4ua.org

ABSTRACT

Estimating the economic impact of the Russia-Ukraine conflict with nightlights data

New data sources have been made available to economists over the last years. By studying and quantifying the (short-term) economic impact of the Russia-Ukraine conflict, this paper presents an empirical application - along with a replicable methodology - designed to quantify, in a causal setting, the impact of natural or artificial localized shocks on local economic activities using night-light luminosity. Moreover, with reference to our specific application to conflict, we discuss how our short-term results serve as a valuable benchmark for analysing the long-term causal effects of military missions on the economic development of conflict-affected countries. Results of the difference-in-differences analysis show that the the conflict had a significant impact on local economic activity, being areas under attack experiencing a decline of night-light luminosity of around 16% at the mean value. The effect is heterogeneous, depending on the intensity of the conflict and the characteristics of the affected areas. Our analysis finds no evidence of recovery in the medium term.

JEL CLASSIFICATION: R11
KEYWORDS: night-lights, difference-in-differences, conflict, satellite imagery

Luigi Buzzacchi
Politecnico di Torino
Department of Regional and Urban Studies and Planning
Turin, Italy
luigi.buzzacchi@polito.it

Antonio Matteo De Marco
Politecnico di Torino
Department of Regional and Urban Studies and Planning
Turin, Italy
antonio.demarco@polito.it

Francesco Luigi Milone
Politecnico di Torino
Department of Regional and Urban Studies and Planning
Turin, Italy
francesco.milone@polito.it

1. Introduction

One of the recent main interests in economic studies is the ex-post assessment of the effects of (endogenous or exogenous) shocks. Among the others, examples can be quantifying the economic impact – e.g., in terms of GDP variations – of specific policies, or resulting from specific infrastructural investments – e.g., the opening of railroads or airports – or consequences of crises, conflicts and natural disasters.

Ex-post evaluations of the effects arising from specific shocks – whether regulatory, infrastructural, or crisis-related – are highly complex. This is due not only to their immediate and often highly localized impacts, but also to their indirect effects, which can extend across broader and less clearly defined areas. Moreover, the effects of a single shock are hard to disentangle, as overlapping shocks often affect neighbouring regions and/or arise in quick succession. For all these reasons, ex-post evaluations may require near real-time data analysis and adequate temporal and spatial granularity to yield meaningful insights. These circumstances were, for instance, relevant during COVID-19 pandemic, when the need to timely track the economic impact of cases diffusion was crucial to plan prospective recovery actions (Hale et al., 2021). Also, the usage of administrative boundaries could fail to capture the relevant spatial unit under analysis. As noted by Go et al. (2022) this can be for instance the case of airports development, where the expected positive effects on flows can be significant only in areas closer to the airport, or, in other words, highly heterogeneous depending on the distance from the (infrastructural) shock.

It is evident that traditional measures such as national accounts (e.g., incomes) or regional outputs (e.g., regional tourism inflows, gross regional products, etc.) do not respect these features, thus constraining researchers' ability to fully comprehend the effects of a specific shock. This paper builds on the recent literature that explores the potential of night-light luminosity data for ex-post shock assessment, in response to the limitations of institutional data.

Despite the advantages and the strong informative value brought by night-light luminosity, scholars have not widely exploited night-light imagery to provide ex-post shock evaluation analyses. The few examples discussed in literature – e.g., Go et al. (2022); Roberts (2021); Roshan et al. (2024); Giovannetti and Perra (2020) – often provide descriptive analyses or just focus on alternative satellite data (e.g., traffic flows), neglecting nigh-light intensity or not treating them appropriately (see the discussion in Gibson et al., 2020). To address this gap, this paper examines the ongoing Russia–Ukraine conflict in order to evaluate the informational value of night-light intensity for interpreting the effects of exogenous shocks on local economic activity. Assessing the socio-economic consequences of such a complex episode, indeed, necessitates: a) timely data to track economic effects in near real time; b) frequent data release, as there can be large variance in economic activity next and far from specific war events; and c) granular information, as war events are highly localized and may trigger spillovers only in nearby areas.

This study contributes along two distinct, yet interrelated, dimensions.

First, from a methodological standpoint, it introduces and examines several challenges in using night-light data to assess the short-term impacts of events that disrupt human activity within a territory, often difficult to be identified, also considering that our case study comprises tens of thousands of military events that impacted Ukrainian territory over a period of three semesters. In this sense we provide a formal assessment of these data in causal inference settings (Roth et al., 2023; Borusyak et al., 2024; Callaway and Sant'Anna, 2021; De Chaisemartin and d'Haultfoeuille, 2024) demonstrating their relevant informative power when higher time frequency is required and in front of complex econometric designs (e.g., *staggered* treatment designs with repeated treatments).

Secondly, our paper aims to contribute to the established literature on the economic effects of conflicts by highlighting the specific and, in our view, significant role that these novel data sources can play. For this purpose, certain essential premises are required.
Wartime events have obvious economic relevance. Poverty often generates conflicts, and conflicts always generate poverty. However, economists have long debated whether the economic effects of wars last in the long run. Neoclassical orthodox models predict that – insofar as the primary impact of conflicts is the destruction of physical and natural assets and a loss, or temporary decline, in human capital investments – *in the long-run* post-war catch-up growth in a Solow framework can restore the economy to its pre-war steady-state equilibrium.
On the other side, starting from Azariadis and Drazen (1990), and then Sachs (2006) threshold poverty trap models account for the contrasting evidence by arguing that, below a certain level of destruction, war-torn societies may settle into a chronic low-growth or stagnation equilibrium for an indefinite period. In this state, individuals and groups remain trapped in persistent poverty, where not only the scarcity of resources—preventing investment—but also the deficiencies in institutions and social capital play a critical and enduring role (Bowles et al., 2011). In other words, threshold poverty traps consequently attempt to explain long-term underdevelopment. It should be noted that these effects often occur in regions that do not align with national borders or precise administrative boundaries, frequently impacting remote and otherwise disadvantaged areas (Kraay and McKenzie, 2014). The empirical evidence of poverty traps, however is still scarce.

Unlike our perspective, the relevant literature on these issues predominantly focuses on long-term horizons. On the empirical side, Davis and Weinstein (2002) and Brakman et al. (2004) study the allied bombing of, respectively, Japanese and German cities in WWII as a shock to relative future city sizes; more recent papers have analysed the bombing campaigns during the Vietnam War, in Vietnam (Miguel and Roland, 2011), Laos (Guo, 2020; Yamada and Yamada, 2021; Riaño and Valencia Caicedo, 2024), and Cambodia (Saing and Kazianga, 2020, and Lin, 2022). Collectively, these findings offer no clear consensus. Davis and Weinstein (2002) and (in part) Brakman et al. (2004) show that even substantial temporary shocks to urban areas do not have a long-term effect on city size; also Miguel and Roland (2011) and Yamada and Yamada (2021) document evidence of catch-up growth; in contrast, evidence of poverty traps appears to emerge in the cases of Laos and Cambodia (Guo, 2020; Saing and Kazianga, 2020; Lin, 2022). Naturally, no

studies on the long-term effects of the Russian-Ukrainian conflict have yet been published. With objectives entirely different from ours, several studies have begun to appear that use general-purpose econometric models to quantify the impact of the war on the global economy (see, e.g., Liadze et al., 2023, and Rose et al., 2023).

The methodology employed in the aforementioned studies relating to the Vietnam War relies on the availability of geo-referenced, comprehensive data on all ordnance dropped by U.S. and allied aircraft and helicopters in South-East Asia between 1965 and 1975, as well as artillery fired from warships. This enables the authors to compare the economic growth of heavily bombed areas with that of less affected regions. The main limitation of this approach lies in the difficulty of isolating the direct – and therefore localized – effects of individual attacks, their short-term persistence, and the interrelation of multiple shocks (military events) that are correlated across time and space. Moreover, even when detailed, bombing data offer only limited insights into the short-term consequences of destruction—such as the loss of value and the resulting decline in production, public services, and daily life, which could otherwise help prevent the onset of a national poverty trap. In the long run, if post-war capital, whether domestic or foreign, proves sufficient, high factor mobility between regions may further obscure localized impacts. Our paper aims to provide short-term (i.e., monthly) measures of the economic effects of conflicts, which may serve as a more appropriate basis than bombing data alone for estimating and localizing long-term (years or decades) impacts.[1]

After methodologically discussing how to implement econometric analyses with these data (e.g., what controls to be included, how to address potential confounds in presence of military events), we show how night-light intensity is highly valuable to study short-run effects of conflict on local economy. We find that following the first attack in a given Raion (a granular Ukrainian administrative area with average surface of about $50km^2$) average night-light decrease by around 16%, with effect that are heterogeneous depending on the intensity of the conflict (i.e., number of military events) and other local controls. The impact is almost immediate and it is persistent in the medium term (i.e., about 1.5 years after the conflict oubreak). Furthermore, we also show, in a *staggered* difference-in-differences setting (Roth et al., 2023), how night-light data works, showing high consistency between canonical methods and novel estimators (Roth et al., 2023).

The final step in our approach is to translate the observed reduction in night-lights into estimates of the decrease of economic activity. This is a critical and non-trivial task: variations in night-light illumination are not linearly proportional to the intensity of military operations – or, for instance, to the magnitude of natural disasters – depending on the degree of anthropization of the affected area. Furthermore, while a reduction in night-lights reflects a general decline in human activity, the resulting economic impact

[1] Yamada and Yamada (2021) also employ night-light data in their study to evaluate the effects of the Vietnam War in Laos. However, the authors use night-light intensity to proxy the long-term effects of U.S. bombing missions on economic development, rather than the short-term impacts on the activities of the affected territories.

varies according to the structure and composition of local economies. In our case, drawing on the estimates of Henderson et al. (2012), we predict a short-term reduction between 10% and 20% in gross domestic product (GDP), which corresponds to about half of the official figures (i.e., -29.2%). We discuss that this evidence suggests that rooted GDP-nightlights elasticity can be way larger in presence of a structural shock (military conflicts) since multiple (complex) economics mechanisms are jointly occurring.

The rest of the paper is organized as follows. In Section 2 we provide a brief overview on the literature dealing with night-light data in economics. In Section 3 we present the data and the variables employed in our analyses. In Sections 4 and 5 we present the identification strategies and the results. Finally, in Sections 6 and 7 we compute the economic translation of our night-light outcomes and we draw conclusions.

2. Literature review

Night-light data are part of the broad family of satellite-derived data. Historically these data have been made available by NASA from 1975 by two different sources: DMSP - Defense Meteorological Satellite Program - up to 2013 and VIIRS - Visible Infrared Imaging Radiometer Suite - from 2011 (see Gibson et al., 2020, for a technical review of literature on these data). Specific features, such as high time-frequency (i.e., they can be observed daily), granularity of spatial- and luminosity-scale (i.e., the raw data, as discussed in the following sections, report a night-light intensity ranging in a scale from 0 to 255 corresponding to a specific pixel covering a $0.5km \times 0.5km$ area) and promptness (i.e., they can be accessed almost in real time) made these new sources of data particularly interesting to researchers that started exploring to what extent night-light luminosity is capable to predict local anthropic activity and, hence, local economic production.

The reminder of this section is as follows. First, we discuss the (increasing) usage of night-light satellite data in economics, depicting pros and features of such data sources. Second, we provide a brief overview on the literature – still flourishing – exploiting these sources as economic outcomes to evaluate the impact of exogenous shocks (e.g., policies, crises, infrastructural developments, and, as in our case, conflict related events).

2.1. On the use of night-light satellite data in economics

As said, in recent years, the increasing availability of digitized satellite imagery has greatly expanded opportunities for empirical research, and among the various sources, images of night-lights have been widely accepted and increasingly used. Historically, these data have been made available by NASA (now through the Earth Observation Data repository[2]), that supplied from 1975 to 2013 data in the format of DMSP (Defense Meteorological Satellite Program), while from 2011 onwards in the VIIRS (Visible Infrared Imaging Radiometer Suite) format.

[2] https://www.earthdata.nasa.gov

As reported by Gibson et al. (2020), several studies questioned the accuracy and the predictive power of such data with the aim of understanding to what extent night-light imagery could be used as a reliable source to address socio-economic related research questions. In this sense, Gibson et al. (2020), by the means of econometric tecniques, showed that VIIRS data are much more accurate than DMSP. In other words, VIIRS have significantly higher predictive power as they explain 80% more of the observed variance than DMSP data to predict some economic variables (e.g., GDP). The latter, in fact, show several limitations, such as blurring, imprecise calibration and truncation of the most extreme data (i.e., *top-coding*).

Grounding of that fact that lights can be a relevant proxy for the presence of anthropic activity, and its intensity over time (Gibson et al., 2020), these have been (recently) used to study a very broad set of economically relevant questions: e.g., where a centre of economic activity in a country is located, how its magnitude/relevance evolves (even in the short term), what effects shocks of various kinds may have in the evolution of anthropogenic activity, or the identification of boundaries, different from administrative ones, of spatial areas that circumscribe the economic practices.

The seminal paper by Henderson et al. (2012) provides one of the most impactful applications of satellite data in economics as they integrate night-light intensity with economic growth indicators all over the globe. They find that the real GDP for 188 countries (1992-2008) responds to changes in average night-light intensity with an elasticity of roughly 0.18–0.32.[3] As discussed in Section 6, it is important to emphasize that the GDP–night-lights elasticity estimated by Henderson et al. (2012) reflects long-run adjustments under normal economic conditions. Conversely, one could argue that the elasticity observed during a shock may reflect fundamentally different dynamics and should therefore be regarded as a measure that is, at least in part, distinct.

Using lights, empirical analyses of growth need no longer to use countries as the unit of analysis: growth for sub- and supranational regions can be measured. For instance, Henderson et al. (2012) evidence shows that in sub-Saharan Africa, coastal areas are growing more slowly than inland regions, which cannot be detected through *traditional* accounts. In the same spirit, Bickenbach et al. (2016) extensively studied the nexus between GDP growth and nigh-light intensity at the sub-national level in emerging economies such as India and Brazil.

Apart from the correlation between night-light and GDP, other questions have been discussed exploiting these data sources. In line with regional economics research, Henderson et al. (2017) exploited night-lights to estimate the role of first nature advantages in determining the worldwide spatial distribution of economic activity, distinguishing between

[3]For countries with poor national income accounts, Henderson et al. (2012) show that the optimal estimate of growth is a composite with roughly equal weights on conventionally measured growth and growth predicted from lights. Their estimates differ from official data by up to three percentage points annually. This result provides an important implication, as it confirms the value of night-light imagery as a substitute (or complement) of national accounts in presence of poor local statistical offices.

advantages for agriculture and those for trade. Briefly, they show, over an analysis of more than 240,000 grid cells, that a significant share of worldwide and within country variation of night-light intensity – and hence of economic activity – is explained by physical geographical attributes. Again, the specific attractiveness of this research relies in the possibility of observing within country variations, linking economic activity with granular physical geographical attributes. Differently, Harari (2020) used night-light imagery to study the causal relationship between urban morphology and cities economic performances. Building on the granular scale of night-light intensity, Harari introduces novel indicators (i.e., shape, compactness, layout) to measure city morphology, overcoming the traditional constraints of administrative boundaries.

Overall, what emerges is that night-light data are a novel and relevant asset for economic studies, which allow researchers a limitless - and still underserved - set of research questions.

2.2. Empirical approaches using night-light satellite data to evaluate exogenous shocks

Few contributions exploited night-light intensity as outcome variables to evaluate the impact of exogenous shocks.

Among the others, Roberts (2021) used night-light imagery to estimate, at the regional and national level, the impact of COVID-19 on Morocco's economic activity. The contribution of Roberts is relevant, as it shows the relevant contribution of night-light data to provide causal assessments of exogenous shocks at higher time frequency – i.e., almost in real time – which is not possible when using traditional national accounts. Following its contribution, a large body of literature exploited these data to estimate the impact of COVID-19 in real time across several geographies.

Go et al. (2022) used satellite data to evaluate the impact of infrastructural shocks – i.e., the opening of a new terminal at the airport of Cebu in the Philippines – comparing night-light luminosity with traffic data (vehicle densities). In the spirit of our work, Go et al. (2022) stress the novelty of satellite imagery to run policy evaluation analyses, that, by definition, in most of the cases need to observe phenomenon with higher time frequency – compared to the release of traditional accounts – and suitable spatial granularity. Particularly, they show that traffic satellite images, as night-light luminosity, are significantly correlated with local economic activity and, in a difference-in-differences setting, they also find that following the infrastructural shock economic activity significantly increases. However, they suggest and offer initial evidence that in economies where tourism plays a major role, night-light data tend to understate actual levels of economic activity.

Closely tied with our research, few studies exploited, with different methodologies, night-light data to assess the economic impact of conflicts. With a descriptive approach, Roshan et al. (2024) analysed the impact of Russia-Ukraine war on surface heating, emissions and night-light. They found a reduction of around 27.2% in 2022 with respect to 2021, which was used as a benchmark. Second, they also provide an heterogeneity analysis based on specific locations, showing a more pronounced decline in Kharkiv and Mariupol. Giovannetti and Perra (2020) used night-lights to assess the effect of Syrian Civil War of

2011, also reporting the corresponding (estimated) loss in GPD through the analysis on night-light luminosity. Particularly, by the means of night-lights and the methodology of Henderson et al. (2012) they predict a loss in Syrian GDP in the range between 34.4% to 43%, while national accounts showed a range between -17% to -25%.

Hence, what clearly emerges from this novel literature is that night-lights offer a novel opportunity to researchers to assess economic phenomenon with all new temporal frequency and spatial granularity, thus addressing a range of empirical limitations inherent in the use of traditional economic indicators.

3. Data sources

To estimate short- and medium-term impacts of the Russia-Ukraine war, we have to exploit data that are: a) released at a high temporal frequency, to distinguish between immediate and long-lasting effects, and b) available at a granular geographical level, to correctly disentangle intensely attacked areas with none or low attacked ones. It is evident, therefore, that relying solely on canonical economic measures is insufficient in this kind of empirical setting. For instance, GDP data, in its most granular form, are available at the region-quarter level only, which is not sufficient to isolate short-term effects from medium term ones. In this context, the use of satellite-based night-light intensity data can be highly effective to overcome these (potential) limitations as these data combine temporal granularity and promptness with a high level of spatial detail (the raw data is indeed available at pixel level, covering a $0.5km \times 0.5km$ area).

The following sub-sections first describe the choice of the spatial level of aggregation, discussing how raw night-light intensity pixel-level information have been aggregated and operationalized in a statistically manageable format. Second, we present the procedure to identify areas under attack (i.e., treatment allocation) and the other data sources employed in the estimation procedure.

3.1. Data sources

3.1.1. Night-light data and choice of the spatial aggregation

To cover a period sufficiently extending back to pre-conflict conditions, needed to correctly extrapolate conflict-induced impacts, monthly VIIRS (Visible Infrared Imaging Radiometer Suite) light data, at the individual pixels level, were extracted from January 2018 to August 2023. These data were derived from the satellite imagery of the NPP (National Polar-Orbiting Partnership) project.[4] The granular specificity of the raw data allows us to decide at what level we can observe the economic phenomenon under examination. Two possibilities are likely at work. On the one hand, granular choices (e.g., pixels or municipalities) would be detailed and precise in the allocation of conflict-data, yet they could suffer severe problems of spatial spillovers (either due to economic reasons, or due to

[4] https://www.earthdata.nasa.gov/data/instruments/viirs.

technical features of the data[5]). On the other hand, we could opt for larger aggregations (e.g., regions), which closely adhere to the idea of a single economic system, yet average over different separated sub-markets.

We opted for the second choice, hence, we aggregated pixel data at the *Raion* level, units (district) which closely resemble the idea of NUTS3 areas, in the middle between municipalities and NUTS2 regions (i.e., *Oblasts*). To avoid endogeneity concerns arising from the non-random nature of administrative boundaries (recently changed with a reform passed on January 2020), we opted for the oldest division. We identified 515 Raions, pertaining to 24 Oblasts, yet we restricted our analysis on the subset of 473 Raions located in 21 Oblasts not under the Russian control (i.e., Raions in the Oblasts of Crimea, Lugansk and Sebastopol City).[6]

The overall Ukraine's territory under our analysis is composed by 4,257,165 pixels, of which about 8.7% belongs to Raions under Russian control. Hence, as reported above, we focused our analysis on the remaining 3,886,981 pixels, for a total of 3,886,981 $\times$ 68 months = 264,314,708 pixel-month observations (mean night-light intensity of 0.66, with a standard deviation of 12.02).[7]

We then aggregated pixel-month observations at the Raion-month level. In doing so, we

[5] First, this granular level often fails to understand the relevant economic market under study as it treats as separated spatial units that are, in essence, under the same economic system. Second, in this circumstance, granular data may be exposed to the specific risk of blooming (or overglow) (Shen et al., 2019). This issue refers to the apparent spread of brightness into adjacent darker pixels caused by the fact that in case of very bright signals, the high value in a given pixel may overflow into adjacent ones.

[6] To be precise, the original Raions' division counted 620 unique areas, divided in 498 *Raions* and 112 *Municipalities (Misto)* or *(Mis'ka Rada)*. The 112 *municipalities* are classified as separate entities at the same administrative level of canonical Raions, yet they are, in essence, the main city of a given Raions (note that not all Raions have the main city recorded as a separate entity). We decided to reorganize the entities in our data, using the following rule: a) if the municipality is in the centre of a Raion and its area is totally included in the corresponding Raion, we annexed the municipality onto the Raion, b) otherwise, if the municipality is sharing only a border with the corresponding Raion, we treated the municipality as separate entity. In Appendix A1 we show two auxiliary examples, showing the allocation processes of municipalities to corresponding Raions.

[7] A first preliminary assessment of the data revealed that 0.13% of pixel-month observations (332,197 obs.) recorded a negative value. This is possibly due to the problem of *airglow* (Uprety et al., 2019; Tveit et al., 2022), which happens when technical instruments record very low night-light signals, such that the corresponding calibration mechanism yields negative values closed to zero. Indeed, the mean value of night-light intensity in these observations is about -0.30, while the median is -0.04. First and 99th percentile are respectively -0.44 and -0.01, with the presence of few outliers in the left part of the distribution (min = -199.71) which skew the mean far from the median and from 0. We also noted that the presence of these negative values is homogeneously distributed over the whole Ukraine's territory, with 459 Raions (about 97%) recording at least one negative pixel-month observation in night-light intensity. This evidence suggests the plausible random allocation of these erroneous observations. Under the assumption that such pixels do not represent areas with tangible night-light intensity, we decided to replace all negative values with 0. Similarly, we identified a negligible share of pixel-month observations (6,152 obs.) with nigh-light intensity above the threshold of 255. Also in this case, we assumed the data to be a coding error, hence we replace the value with the maximum possible level, 255.

Table 1: Descriptive statistics: night-light intensity ad Raion level.

Variable	Variable Description	Mean	SD	Min	Max	1st	5th	25th	50th	75th	95th	99th
$DensLight_{it}$	Total light in Raion i at month t per unit of surface.	6.864	21.225	0.000	681.257	1.125	1.693	2.512	3.317	4.836	13.376	95.913
$MedLight_{it}$	Median night-light intensity of pixels located in Raion i at month t.	0.739	2.616	0.000	95.590	0.110	0.210	0.310	0.400	0.550	1.020	10.280

Notes: Descriptive statistics obtained on 32,164 Raion-month observations. 1st, 5th, 25th, 50th, 75th, 95th and 99th are the percentiles of the corresponding variable's distribution.

computed the following two metrics: a) $DensLight_{it}$, equivalent to the sum of night-light intensity of all pixels located in a Raion i normalized by its surface (same as the specification used by Henderson et al., 2012), b) $MedLight_{it}$, the median value of night-light intensity. Table 1 reports the descriptive statistics for the corresponding variables.

To corroborate the informative value of night-light data as *good* proxies of local economic production, in Appendix A2 we show the univariate correlation between night-light density in 2019 and gross regional product at the Oblast level. We find (as expected) a positive and significant relationship (Pearson Correlation $\rho = 0.71$) between the two variables.[8]

3.1.2. Identification of Raions under attack

In order to assess the impact of military attacks on night-lights, and hence on local economic activity, is essential to rely on a representative dataset of conflict-related events in order to distinguish between areas which have been directly involved into the conflict and areas which have not been directly under attack. In this sense, the VIINA (Violent Incident Information from News Articles) dataset offers a valuable source of information. The VIINA dataset tracks, in real time, any type of 'violent' military event, thereby ensuring a comprehensive, undistorted reconstruction of the conflict's timeline.[9] Events are clustered using geocoding dictionaries (allowing for the attribution of geographic coordinates when specific locations are mentioned in news reports).[10] The data is categorized according to

[8] Note that we use data on Gross Regional Product (GRP) at 2013. We find that the univariate regression coefficient, estimating GRP on night-light intensity in a *log-log* specification is equivalent to $+0.74$ (std. err. $= 0.16$, $p < 0.001$), confirming that there is a strong positive correlation between the two measures. Furthermore, this estimate is also robust to the omission of the Oblast of Kiev City, that is an outlier concerning both night-light intensity and GRP.

[9] See https://github.com/zhukovyuri/VIINA. This source's continuous monitoring is based on information provided by both Ukrainian and Russian local media outlets. Some examples are: Ukrainian daily *Ukrayins'ka Pravda*, the *24tvua* network, the live event mapping platform *liveuamap*, and major Russian media outlets such as *Meduza*, *MZ*, and *NTV*.

[10] For the sake of clarity, in its raw form, the VIINA dataset includes a significant number of duplicated events, which arise when two or more media sources report on the same incident, or when the same source issues follow-up reports or updates. The VIINA project offers a revised version of the dataset, cleansed of duplicates through both automated queries and manual verification processes. To construct our metrics

Table 2: Raions by number of military events.

# of events	# of Raions	%	# of military events	Avg. pop. density	Median pop. density	Avg. GRP	Median GRP	Median $DensLight_{2019}$	Median $MedLight_{2019}$
0	135	28.54%	0	38.49	36.67	26,267	28,250	2.94	0.37
1-5	105	22.20%	261	36.75	32.62	25,832	24,160	3.07	0.38
6-10	27	5.71%	214	33.58	30.70	28,258	28,173	3.06	0.37
11-20	23	4.86%	373	44.99	37.04	27,058	28,173	3.53	0.40
21-50	29	6.13%	897	38.16	32.86	32,193	30,095	3.25	0.39
51-100	36	7.61%	2651	87.36	46.97	69,684	28,173	4.37	0.42
101+	118	24.95%	146,943	128.48	48.42	37,645	30,095	4.02	0.41
Total	473	100%	152,384	67.55	37.75	36,873	28,173	3.16	0.45

Notes: a) Population density computed using data at the national census of 2013, b) GRP stands for Gross Regional Product, as is computed by splitting the gross product at the Oblast level (in 2013) proportionally to Raions' population, c) GRP is measured in local currency (UAH), d) Anti-air defence military events are excluded from the count of military events.

the nature of the attack, the involved actors, and the targeted objectives (e.g., attacks on residential buildings or medical zones).[11] In this study, we relied on the number of 'military' events registered in a Raion (or Oblast) i at year-month t, excluding events related to anti-air defence.

Tables 2 and 3 show the distribution of military events among Raions; there is clearly considerable variation in the number of military events per Raion. Overall, 135 out of 473 Raions (28.54%) remained unaffected, while the remaining 338 Raions (71.67%) experienced at least one military event (as of August 2023, the cutoff date of our database), with 118 Raions counting more than 100 events over the sample periods. The 135 Raions that were never attacked will hereafter serve as the *control group*, while the remaining 338 will constitute the *treated group*, as the empirical analysis will focus on *(a)* assessing mean differences in night-light before and after the conflict outbreak in treated versus control Raions and *(b)* assessing the elasticity of night-light to the number of military events (i.e., in a *continuous treatment* model). Concerning the timing of the events (see Table 3), we are in front of a *staggered* roll-out as treated Raions are not treated simultaneously.[12]

concerning the number of military events per each geographical unit, we exploited the cleaned version of the data.

[11] There are different types of attack registered in the VIINA dataset, varying from *'heavy'* event like airstrikes, bombings, armed confrontations, explosives, artillery strikes, heavy vehicle assaults (such as tank operations), special forces actions, to 'other' types of events like cyberattacks, Russian troop withdrawals, occupation of buildings by armed militias, arrests by security forces, or prisoner detentions.

[12] Staggered designs are quite popular in economic research, particularly thanks to the methodological advancements in the econometric literature (Roth et al., 2023; Borusyak et al., 2024; Callaway and Sant'Anna, 2021). Either before or after these methodological innovations, several studies, in fact, have been conducted in various fields of economics using this identification strategy. For instance, in the field of economics of innovation Koenig (2023), Fenton and Koenig (2025), Berger et al. (2018) or Burtch et al. (2018) used the staggered roll-out of TV in the US to estimate the effect of technological shocks on labor supply, *superstars* earnings and conventional incumbents and entrepreneurial activity. In a different field (i.e., health economics), Braghieri et al. (2022) exploited the staggered roll out of Facebook to estimate the effects of social media on students mental health. Differently, Nagengast and Yotov (2025) exploited the staggered design in presence of structural gravity model, suggesting that former estimates

Table 3: Raions by date of first military event.

Time of first attack	# of Raions	%	Cum. %	Avg. pop. density	Median pop. density	Avg. GRP	Median GRP
February 2022	156	32.98%	32.98%	118.59	46.77	41,831	28,520
March 2022	91	19.24%	52.22%	41.57	31.21	31,732	28,520
April 2022	28	5.92%	58.14%	35.69	22.76	27,237	27,517
May 2022	9	1.90%	60.04%	41.78	46.25	30,868	30,095
June 2022	9	1.90%	61.95%	41.39	27.54	28,199	26,860
July 2022	9	1.90%	63.85%	35.93	41.58	26,273	24,161
August 2022	5	1.06%	64.90%	25.24	22.07	31,823	30,095
September 2022	1	0.21%	65.12%	19.32	19.32	30,095	30,095
October 2022	9	1.90%	67.02%	33.62	30.70	20,983	18,896
November 2022	9	1.90%	68.92%	31.51	31.62	23,067	22,324
December 2022	3	0.63%	69.56%	41.70	28.34	22,562	21,775
January 2023	2	0.42%	69.98%	30.99	28.31	23,991	21,158
February 2023	1	0.21%	70.19%	21.48	21.48	30,095	30,095
March 2023	1	0.21%	70.40%	15.16	15.16	18,155	18,155
June 2023	1	0.21%	70.61%	23.11	23.11	37,619	37,619
July 2023	2	0.42%	71.04%	38.93	38.86	18,896	18,896
August 2023	2	0.42%	71.46%	54.47	52.91	22,324	22,324
Never Attacked	135	28.54%	100.00%	38.49	36.67	26,267	28,520
Total	473	100.00%	100.00%	67.55	37.75	36,873	28,173

Notes: a) Population density computed using data at the national census of 2013, b) GRP stands for Gross Regional Product, as is computed by splitting the gross product at the Oblast level (in 2013) proportionally to Raions' population, c) GRP is measured in local currency (UAH), d) Anti-air defence military events are excluded from the count of military events.

Indeed, while almost half of them (156) counted the first military event in February 2022 (i.e., the month in which the conflict officially started), the remaining 182 Raions received the first attack from March 2022 up to August 2023. Nonetheless, in the first 4 months of the conflict, around 60% of Raions were actually treated. Figure 1 reports the map of Ukraine's Raions by number of military events. As shown, the most impacted Raions are those close to the border, whereas the inner and western part of the country are, on average, less interested by military events (except some special cases).

The descriptive evidence presented in Tables 2, 3 and Figure 1 describes the main socio-economic characteristics of Raions interested by military conflicts. On average, we find that treated Raions exhibit larger population density and per capita gross regional product, suggesting that attacks have been located in regions containing densely inhabited cities or industrial areas, mostly located close to the border. This is even confirmed by the fact that the median value of population density and GRP (not biased by the presence of peaks attributed to large cities within groups' distribution) is, instead, less heterogeneous. On the temporal variation of military events, we denote that such densely inhabited and productive Raions have been those first involved in the conflict, even though, also in this

of Regional Trade Agreements could be downward biased if not accounting for the staggered treatment intervention timing. Regardless the sector of study, what clearly emerges is that this empirical situations allows researchers to identify causal relationships, particularly under the robust estimations allowed by the newest estimators (Roth et al., 2023).

Figure 1: Raions by number of military events

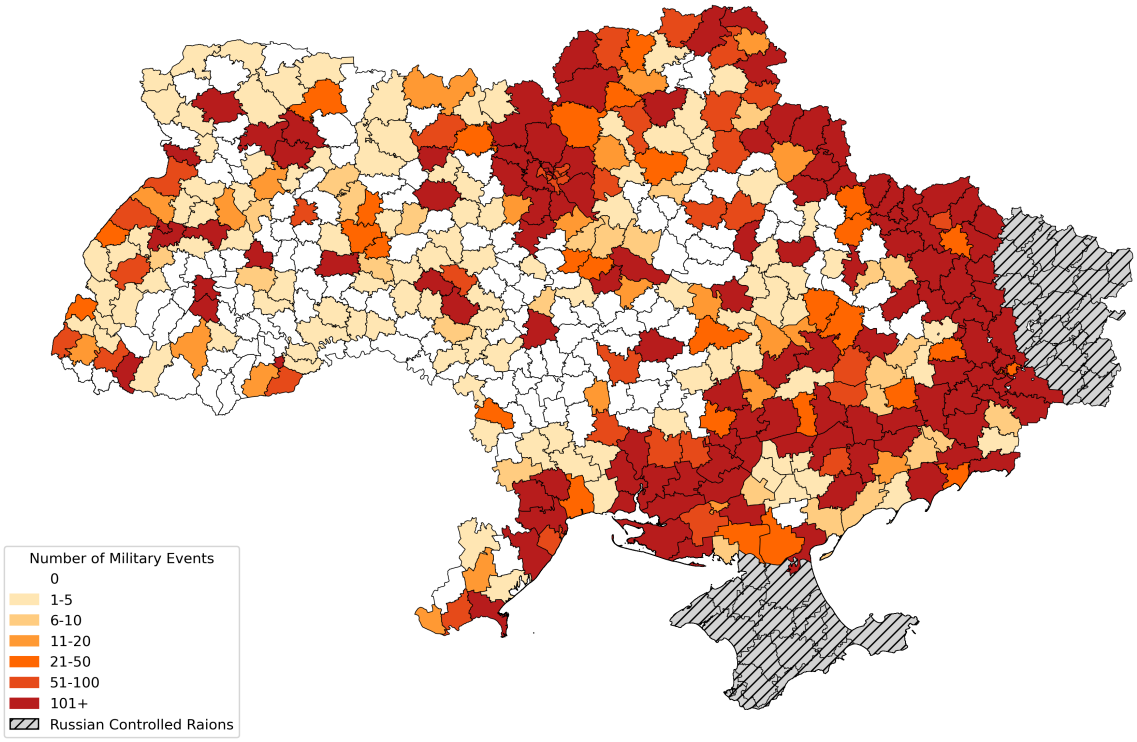

Notes: a) The Raions in the regions of Crimea, Lugansk and Sebastopol City are excluded, b) Anti-air defence military events are excluded from the count.

case, there is not a clear pattern when looking at median values of population density and GRP.

3.1.3. Control variables

A key limitation of night-lights satellite data is the absence of filtering mechanisms or masks applied to the raw data, which may result in inaccuracies due to factors such as cloud cover, diffuse lighting, lunar phases, and other environmental conditions that could skew some observations. Furthermore, the special case of this study (i.e., a war conflict) issues other special conditions which deserve to be further investigated. To this end, we now discuss the specific controls we included in our econometric models.

Fire-related controls.
First, it would be overly simplistic to assume that military attacks, having a negative impact on local economic activity, are determinants of negative fluctuations in night-light patterns. Indeed, fire incidents, are in this case a relevant confounding factor: as a result of an airstrike, in fact, fires may spread. However, these are also correlated with our dependent variable (night-light intensity), not because they have direct effect on economic activity, yet because fire radiative power may have a positive contribution to satellite

detection. This problem could result in biased estimates, as fire radiative power may counterbalance eventual detrimental effects of military attacks on economic activity (hence on night-light). To deal with this aspect, we exploited data from the Fire Information for Resource Management System (FIRMS) developed by NASA, which uses imagery from the VIIRS, MODIS, and Landsat satellites to create daily global maps of active fires.[13] Each active fire is precisely geolocated using geographic coordinates, enabling the integration of fire data within Raions boundaries. Accordingly, we computed the mean fire radiative power (in MW) of fireplaces located in each Raion i in months t.

Anti-air attack defence.
Second, one of the most relevant countermeasures to airstrikes is turning off the lights in a preventive manner. Conceptually, and in econometric terms, this would mean that (almost) systematically, before an airstrike event, the observed night-light intensity should decrease, with no tangible correlation with local economic activity. In a treatment-effect setting like ours, this issues poses challenges to both the fulfilment of the parallel trends assumption, and the absence of anticipatory effects. Without properly dealing with this aspect, indeed, our estimates would be, again, biased. Hence, we counted per each Raion-month the number of anti-air defence military events.

Meteorology controls.
Finally, specific meteorological conditions can exogenously skew the observed night-light value. In this study, we followed a canonical approach in the literature, by controlling for observed weather conditions at the Raion-month level. We gathered from the Copernicus program[14] open data on weather conditions, then aggregated at our level of observation. Specifically, we measured: *(a)* mean temperature (in Kelvin degrees), *(b)* mean rainfalls, and *(c)* mean wind speed.

Table 4 reports the descriptive statistics from our sample, together with a synthetic description of the main independent and control variables[15].

4. Estimation Strategy and Baseline Results

4.1. Estimation strategy

We approached the formal econometric analysis in several complementary ways. Our objective is to estimate the average *direct* impact and persistence of the treatment – namely, the occurrence of military events – on *local* socio-economic activity, proxied by night-light intensity.

[13] https://firms.modaps.eosdis.nasa.gov.

[14] https://www.copernicus.eu.

[15] It is worth to note that we have a full balanced panel (32,164 obs. = 68 months × 473 Raions) when variables concerning military events and fire radiative power are used. When we also include meteorology controls, we lose 1,020 observations pertaining to 15 Raions (13 of them treated, 2 never attacked). We have done ad hoc robustness tests in the econometric analyses replacing the missing value of such a variable with the mean weather conditions of nearby (i.e., contiguous) Raions, and we did not detect significant differences compared to the main results.

Table 4: Descriptive statistics: military events and control variables.

Variable	Description	Source	Count	Mean	Median	SD	Min	Max
$Events_{it}$	Number of military events (excluding anti-air attack defence ones) in Raion i at period t.	VIINA	32,164	4.71	0.00	37.69	0.00	1,226.00
$Conflict_{it}$	Dummy equals to 1 for treated Raions after the first military event (excluding anti-air attack defence ones).	VIINA	32,164	0.18	0.00	0.39	0.00	1.00
FRP_{it}	Average fire radiative power in MW of fireplaces located in Raion i at period t.	FIRMS (NASA)	32,164	3.07	1.37	4.73	0.00	141.22
$Temperature_{it}$	Average mean temperature in Kelvin in Raion i at period t.	COPERNICUS	31,144	283.25	283.32	8.86	264.72	299.34
$Rainfalls_{it}$	Mean total rainfalls in mm in Raion i at period t.	COPERNICUS	31,144	53.37	46.53	33.10	0.21	308.31
$WindSpeed_{it}$	Mean windspeed in m/s in Raion i at period t.	COPERNICUS	31,144	3.42	3.40	0.60	1.21	6.55
$AntiAirDefence_{it}$	Number of anti-air attack defence events in Raion i at period t.	VIINA	32,164	0.25	0.00	2.16	0.00	100.00

Notes: a) Descriptive statistics obtained on 32,164 Raion-month observations, yet in 1,020 observations (15 Raions) we do not have meteorology controls; b) in one case, a negative value in the variable $Events_{it}$ is registered when Anti Air defence events overcome the number of *offensive* military events: we replaced this value with 0.

In the first (static) analysis, we compare the effects of the treatment on Raions exposed to military events (from the date of their first occurrence) with the outcomes observed in Raions that remain untreated or have not yet experienced such events. We propose a difference-in-differences (hereafter DID) estimator using a Two-Way Fixed Effects (hereafter TWFE) regression as follows:

$$Y_{it} = \alpha_i + \beta\, Conflict_{it} + \gamma\, X_{it} + \tau_t + \varepsilon_{it} \tag{1}$$

In our preferred specifications, we tested as dependent variable Y_{it} the night-light density in Raion i at month t ($DensLight_{it}$).[16]

The definition of the dummy $Conflict_{it}$, indicating the treatment status of a given Raion in a month, deserves further discussions. In our setting, indeed, $Conflict_{it}$ takes the value of 1 for treated Raions, after receiving the first attack, 0 otherwise, letting Equation 1 resemble to a *staggered difference-in-differences* design (Callaway and Sant'Anna, 2021; Borusyak et al., 2024; Roth et al., 2023), as treated units are treated at different points in time. It is worth to note that in this specification the estimation of the average treatment effect (β) could be exposed to the issues of a) *negative weights* and cohort-heterogeneous effects (Sun and Abraham, 2021), and b) possible anticipatory effects (even due to spatial spillovers). Hence, we will provide a careful evaluation of alternative estimators according to the recent econometric literature which suggests specific models to deal with these

[16]However, throughout the entire analysis, we will also present several robustness checks using median ($MedLight_{it}$).

issues of the staggered design (Borusyak et al., 2024; Callaway and Sant'Anna, 2021; Roth et al., 2023; De Chaisemartin and d'Haultfoeuille, 2024).

X_{it} is the set of control variables. As previously discussed, we include a rich set of meteorological controls: average temperature in linear and quadratic term, mean rainfalls and average wind speed. Furthermore we notably control for mean fire radiative power of fireplaces detected in Raion i at time-period t and for the count of anti-air defence events. All control variables, except the mean fire radiative power, are transformed using the *asinh* transformation. α_i and τ_t are respectively Raion and year-month (i.e., time) fixed effects, respectively capturing cross-sectional differences across Raions and common (macro-economic) shocks to all Ukraine.

The key identification assumption is the fulfilment of the parallel trends assumption (Roth et al., 2023). That is, in absence of localized military events, night-light intensity in treated and never (or not-yet) attacked Raions would have evolved in a similar pattern. Put differently, trends in night-light intensity before the first military event registered in a Raion i are not statistically different from those of *control* Raions. Figure 2 reports the evolution of mean $DensLight_{it}$ (in levels and *asinh* transformed) by period, distinguishing between treated and control Raions.[17] Here, the control group is composed by all Raions not yet treated at the corresponding point in time, while, treated groups are distinguished by cohort. For the sake of clarity, given they are the most relevant in terms of number of Raions, only the cohorts of February, March, April and May 2025 are shown. It emerges that up to January 2022 (the vertical reference line), the temporal pattern describing the evolution of night-light intensity is similar comparing the various treatment cohorts and the control ones. In levels, instead, we denote that the earliest treated group (i.e., February 2022) shows a systematically higher intensity compared to control and late treated groups. Notably, following the beginning of the conflict there is a decline of $DensLight_{it}$ across all groups, suggesting that the conflict generated a negative shock on the whole country, regardless the fact that the Raion was attacked or not.[18] Contrary to our guesses, we also denote that in control Raions the downward trend following the conflict outbreak seems larger than those in the treated groups. This suggests – apparently – that in conflict area night-light intensity decreased less than proportionally compared to the control group. However, it is worth to mention that the presented statistics are univariate, and do not control for relevant confounds, such as fireplaces and anti-air defence events, which are likely to affect the observed night-light in treated Raions.

Nonetheless, to provide a careful inspection of parallel pre-trends, we will also resort to an event study specification with leads and lags to the onset of the first military event as follows:

[17] In Appendix A3 we report the same figures with $MedLight_{it}$.

[18] In this sense, the inclusion of year-month (i.e., time) fixed effects is rather effective to control for such a common shock to all spatial units in our data.

Figure 2: Evolution of $DensLight_{it}$ over time

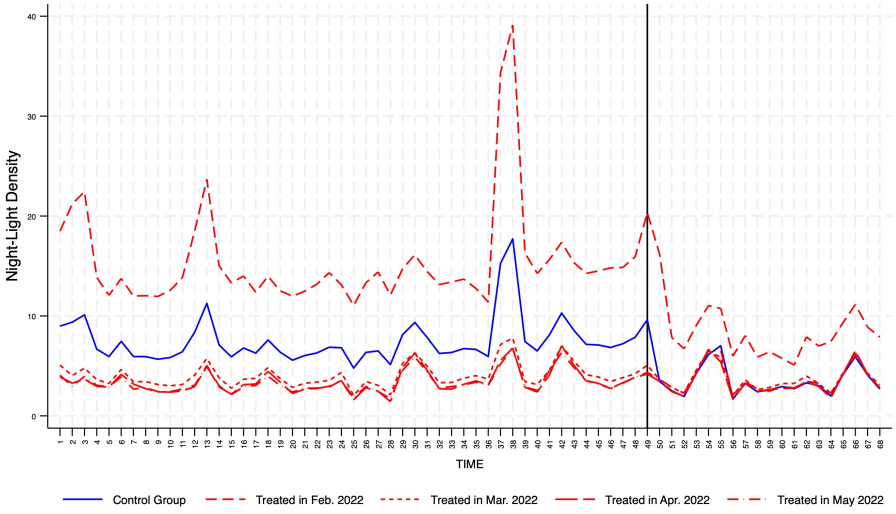

(a) y = $DensLight_{it}$

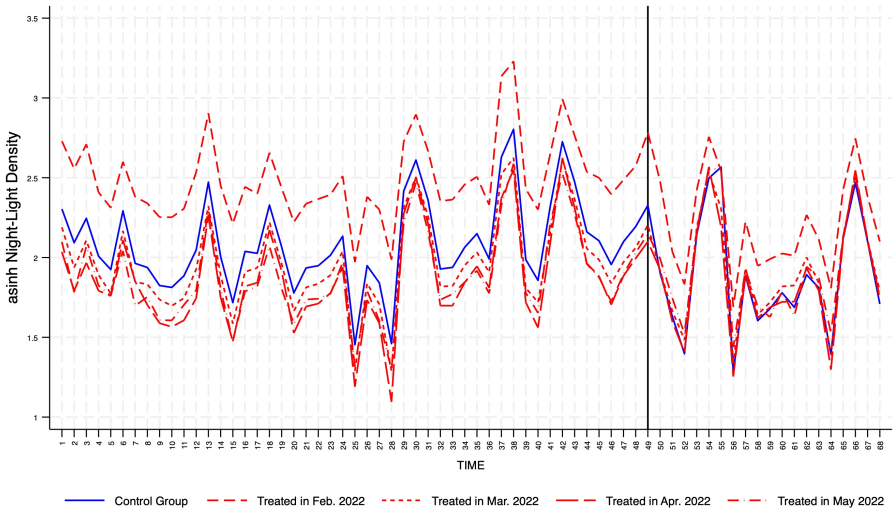

(b) y = $asinh\ DensLight_{it}$

Notes: a) group mean value is shown, b) control group contains Raions not yet treated at the corresponding point in time (hence both never treated and not yet ones), c) the four largest treatment cohorts are shown; d) vertical reference line T = 49 = January 2022 (one period before conflict begins).

Table 5: Baseline TWFE estimates.

	$\mathbf{y} = DensLight_{it}$			$\mathbf{y} = \boldsymbol{asinh}\ DensLight_{it}$		
	M1.1	**M1.2**	**M1.3**	**M2.1**	**M2.2**	**M2.3**
$Conflict_{it}$	-1.498***	-1.690***	-0.707***	-0.144***	-0.105***	-0.088***
	(0.363)	(0.599)	(0.237)	(0.021)	(0.019)	(0.018)
$asinh\ Temperature_{it}$	-6480.891***		-7045.070***	-859.628***		-909.596***
	(2452.830)		(2611.185)	(104.262)		(103.684)
$asinh\ Temperature_{it}^2$	507.468***		551.992***	67.365***		71.316***
	(192.416)		(204.889)	(8.216)		(8.169)
$asinh\ Rainfalls_{it}$	-0.011		0.021	-0.011***		-0.010***
	(0.024)		(0.035)	(0.003)		(0.003)
$asinh\ WindSpeed_{it}$	-0.492**		-0.260	-0.102***		-0.085***
	(0.214)		(0.227)	(0.025)		(0.024)
FRP_{it}		0.041***	0.013*		-0.001**	-0.000
		(0.013)	(0.006)		(0.000)	(0.000)
$asinh\ AntiAirDefence_{it}$		-3.994**	-1.868**		-0.133***	-0.132***
		(1.668)	(0.849)		(0.028)	(0.030)
Constant	20696.215***	7.372***	22482.763***	2744.453***	2.096***	2902.423***
	(7816.614)	(0.107)	(8318.981)	(330.756)	(0.004)	(329.005)
Raion FE	Yes	Yes	Yes	Yes	Yes	Yes
Time FE	Yes	Yes	Yes	Yes	Yes	Yes
N	31,144	32,164	31,144	31,144	32,164	31,144
R2	0.717	0.797	0.726	0.834	0.896	0.840
Within R2	0.012	0.028	0.044	0.032	0.061	0.071

Notes: a) *** p<0.01, ** p<0.05, * p<0.10, b) clustered standard errors at the Raion level in parentheses.

$$Y_{it} = \alpha_i + \sum_{\substack{k\in[-G;M]\\ k\neq -1}} \nu_k\ E_{i,t+k} + \gamma\ X_{it} + \tau_t + \varepsilon_{it} \tag{2}$$

where, $E_{i,t+k}$ are binary lead and lag terms capturing a given number of periods (months) k before and after the timing of the military event in a Raion i and ν_k are the corresponding estimates of the *dynamic* treatment effect. The first lead ($k = -1$) is normalized to zero following standard practice. G and M represent the maximum leads and lags observable in our specifications, with $G = 67$ and $M = 18$.

4.2. Baseline TWFE estimates

Table 5 presents the estimation results for the static DID designs using a canonical TWFE estimator. In all regressions, the average treatment effect associated to the variable $Conflict_{it}$ is always negative and statistically significant. This evidence suggests that following the first military events, the decrease in night-light intensity in treated Raions was larger than the one in control Raions. Overall, we estimate that treated Raions experienced an average decline ranging from -1.690 to –0.707 in levels. In relative terms (see models M2.1 to M2.3) we estimate an elasticity of night-light intensity to conflict

outbreak in the range between -13.4% and -8.42%.[19,20]

Rather interestingly, the magnitude of the estimated average treatment effect varies depending on the inclusion of specific controls. This suggests that the presence of omitted confounds correlated with $Conflict_{it}$, and positively/negatively correlated with our dependent variable is remarkably important. $AntiAirDefence_{it}$ represents a strongly significant predictor of night-light intensity as we estimate an elasticity of -0.132 (in other terms, doubling the number of air attack defence events decreases night-lights on average by 8.7%[21]). This is in line with ex-ante expectations: in presence of such mechanisms, average night-light intensity should decrease. The presence of fireplaces, and the corresponding fire radiative power, has a mixed evidence. In levels (models M1.2 and M1.3), we find, as expected, a positive correlation between fire radiative power and night-light density. Temperature is found to be negatively correlated with night-light density with diminishing (negative) returns. Also, wind speed and rainfalls are both negatively associated with night-light, further confirming the need of correctly adjusting satellite raw data to weather conditions.[22]

4.3. Specific estimators for staggered difference-in-differences design and event study estimates

As mentioned in Section 3, the nature of our analysis, studying a treatment allocated at different point in times to different Raions, requires specific methodological approaches (Roth et al., 2023). Without proper methodological choices, our analysis can be, indeed, exposed to the issue of *forbidden comparisons* (Goodman-Bacon, 2021): late treated Raions may be – erroneously – compared to early treated ones in order to derive a single weighted

[19] Elasticities computed as $e^{\beta} - 1$. This means that we estimate a decline in treated Raions, following the first military event ranging between -8.42% and -13.4% compared to counterfactual outcomes (i.e., treated Raions with no treatment allocation).

[20] In Appendix A4 we provide the same estimates using $MedLight_{it}$ as dependent variable showing rather similar results in terms of sign and significant. It is worth to mention that when $MedLight_{it}$ is used as dependent variable, our estimate is in magnitude lower. Nonetheless, we return in Section 5.2 on this.

[21] Elasticity computed as $2^{-0.132} - 1 = -0.087$.

[22] It is worth to mention that all our estimates include year-month fixed effect, which naturally control for the presence of heterogenous seasonal effects. Nonetheless, the observed correlation between night-light intensity and meteorological controls could still be driven by local season-related unobserved confounds. Hence, in Appendix A5 we test an additional specification where we absorb an additional level of fixed effects, controlling for Oblast times season (i.e., winter, spring, summer, autumn) effects (in models M1 to M4) or Raion times season effects (in models M5 to M8). We see that the estimated negative relationship – with diminishing returns – between night-light intensity (either using density or median) and the negative effects of rainfalls and wind-speed (only when using the *asinh* transformation) are robust to the inclusion to such additional effects. This evidence confirms that such controls capture specific variations in night-lights, instead of spurious correlations. Since the estimated average treatment effect is rather similar (e.g., $\beta = -0.084$ when using *asinh* $DensLight_{it}$ as dependent variable), we will discuss in the following sections only models absorbing Raions and year-month fixed effects.

average treatment effect, hence biasing (upward or downward, depending on the real effect of the treatment) the overall estimate.

It is true that in this specific empirical setting ex-ante expectations tend to suggest that the exposure to such an issue is limited: as reported in Table 2, in fact, almost all treated Raions have been treated within the first four months of the conflict (February-May 2022), reducing the relative importance of the *forbidden comparisons*. Furthermore, in Appendix A6, we also show the weighted decomposition of the average treatment effect according to Goodman-Bacon (2021). In line with the large concentration of treatment allocations between February 2022 to May 2022, we evidence that most of the estimated average treatment effect from canonical TWFE models comes from the (good) comparison between treated and never treated Raions, hence revealing that the issue of *forbidden comparisons* is relatively moderate in our setting. Nonetheless, to get unbiased estimates, particularly in an event study approach, we resort to the estimators of Borusyak et al. (2024) (BJS) and Callaway and Sant'Anna (2021) (CS).[23]

Table 6 reports the estimate. We confirm that our estimates are fairly robust to those reported in Table 5 using canonical OLS TWFE method. To be precise, we note that TWFE tends to underestimate the average treatment effect evidenced by both BJS and CS. Both estimators, indeed, show a more pronounced decline in night-light intensity, with an estimated elasticity, using the most complete specifications (M2.3 and M4.3) rather similar and around -16.00%.[24] The evidence is convincing: in fact, the presence of *forbidden comparisons* comparing late attacked Raions with those already attacked (and which already experienced a decline in night-light intensity) may produce positive estimates, which downward bias the overall average treatment effect. Although overall negligible, both BJS and CS prevent from such a bias.[25]

The previous analyses offer a static view on the impact of the conflict on night-light intensity. Figure 3 provides, instead a dynamic view, by the means of an event study plot, which allows for considerations on the short- and medium-term impacts.[26] Several

[23] These estimators are suitable for the staggered treatment adoption, yet they work differently. Borusyak et al. (2024) propose an *imputation* estimator. Specifically, they fit a first-stage TWFE regression using observations only for units and time periods that are not-yet-treated. Then, they estimate the never-treated *potential* outcome for each treated unit exploiting the first-stage fitted model, and compute individual treatment effect for each treated unit as the difference between observed and fitted values. Such individual effect is then aggregated to compute the average estimated effect. Callaway and Sant'Anna (2021)'s estimator, instead, works differently, as it provides a weighted average of all possible comparisons (excluding the forbidden ones), allowing the researchers to select as control group either never-treated units or not-yet treated ones.

[24] Computed as $e^{-0.171} - 1 = -15.71\%$ for BJS and $e^{-0.178} - 1 = -16.30\%$.

[25] In Appendix A7 we show the same estimates using $MedLight_{it}$ and its *asinh* transformation as dependent variables. As per the canonical OLS TWFE estimates, the results are robust in terms of sign and significance, while in (absolute) magnitude are lower. Again, in Section 5.2 we provide an explanation on this.

[26] By construction, the event study plot employs a relative time to treatment time axis. Time equals to 0 corresponds to the first month in which the Raions received a military event, time equal to +/- 1

Figure 3: Event study estimates with y = $asinh\ DensLight_{it}$.

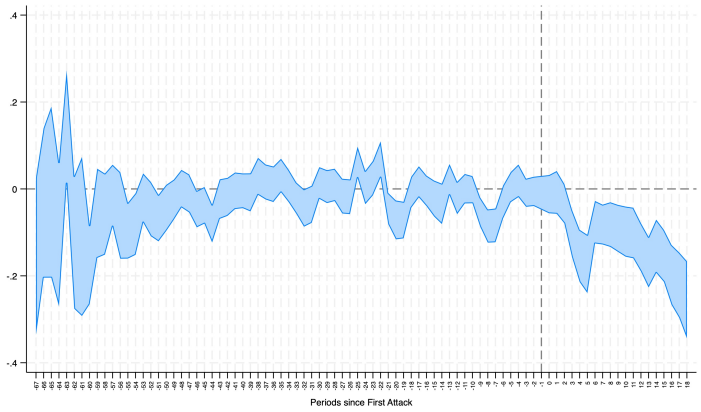

(a) Canonical TWFE estimator.

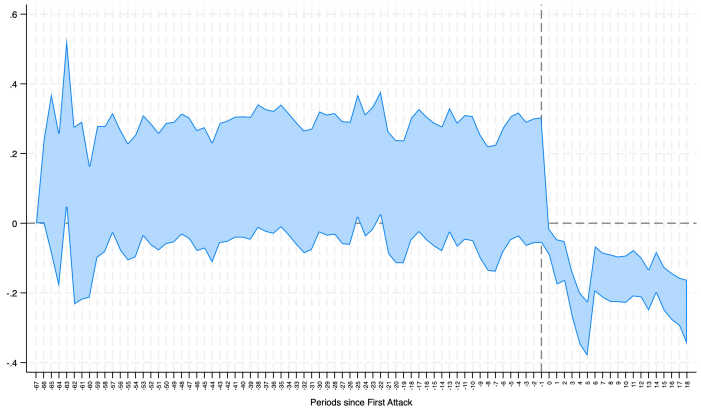

(b) Borusyak et al. estimator.

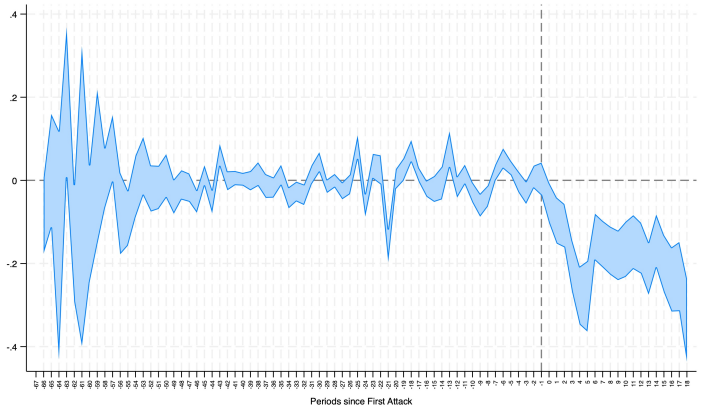

(c) Callaway & Sant'Anna estimator.

Notes: a) 95% confidence interval based on clustered robust standard errors at the Raion level is shown; b) the vertical line (dash line) refers to one month before the treatment (i.e., first military event).

Table 6: Estimates with estimators for staggered design.

	Borusyak et al. - BJS					
	y = $DensLight_{it}$			y = $asinh\ DensLight_{it}$		
	M1.1	**M1.2**	**M1.3**	**M2.1**	**M2.2**	**M2.3**
$Conflict_{it}$	-1.619***	-3.864***	-1.691***	-0.157***	-0.190***	-0.171***
	(0.380)	(0.878)	(0.398)	(0.022)	(0.029)	(0.029)
Controls *weather-related*	Yes	No	Yes	Yes	No	Yes
Controls *conflict-related*	No	Yes	Yes	No	Yes	Yes
RaionFE	Yes	Yes	Yes	Yes	Yes	Yes
TimeFE	Yes	Yes	Yes	Yes	Yes	Yes
N	31,144	32,164	31,144	31,144	32,164	31,144
	Callaway & Sant'Anna - CS					
	y = $DensLight_{it}$			y = $asinh\ DensLight_{it}$		
	M3.1	**M3.2**	**M3.3**	**M4.1**	**M4.2**	**M4.3**
$Conflict_{it}$	-2.600***	-5.896*	-2.599***	-0.180***	-0.211***	-0.178***
	(0.606)	(1.358)	(0.605)	(0.029)	(0.029)	(0.028)
Controls *weather-related*	Yes	No	Yes	Yes	No	Yes
Controls *conflict-related*	No	Yes	Yes	No	Yes	Yes
Raion FE	Yes	Yes	Yes	Yes	Yes	Yes
Time FE	Yes	Yes	Yes	Yes	Yes	Yes
N	31,144	32,164	31,144	31,144	32,164	31,144

Notes: a) *** p<0.01, ** p<0.05, * p<0.10, b) clustered standard errors at the Raion level in parentheses, c) BJS stands for Borusyak et al. (2024) estimator, d) CS stands for Callaway and Sant'Anna (2021) estimator and employed not-yet treated Raions as control group; e) Controls *weather-related* contains: $Temperature_{it}$ (in linear and quadratic terms), $Rainfalls_{it}$ and $WindSpeed_{it}$; f) Controls *conflict-related* contains: FRP_{it} and $AntiAirDefence_{it}$.

considerations can be done. First, regardless the estimators, all specifications highlight the absence of a recognizable path prior to the allocation of the event. In all cases, indeed, the average treatment effect (before the first military event) is located around zero. In OLS (canonical TWFE) and BJS, leads coefficient are also almost never statistically significant, while in CS, despite we have some significant leads, the pattern is clearly not following a specific trend. According to Freyaldenhoven et al. (2021), this is typically a visual assessment of the fulfilment of the parallel trends assumption, which reinforces the validity of DID estimates. Second, in line with the static models, we document a significant drop (below zero) of the average treatment effect following the conflict outbreak. When looking at the results produced by staggered DID estimators (BJS in panel *b* and CS in panel *c*), the effect seems to be almost instantaneous, as we document a drop at the time of the first attack. In the following months, we see that up to six months following the first military

corresponds to one month after/before the first military events, and so on. Given the staggered nature of our design, it is worth to mention that the number of observations available to estimate corresponding dynamic treatment effects at each lead (i.e., periods before the treatment) and lags (periods after the treatment) varies. For instance, to estimate very long distance leads (e.g., T = -67) we can use only the few Raions treated almost at the end of our panel. This is the reason why standard errors are rather large on the left part of the event study plot, while it becomes narrower when estimates get closer to the treatment allocation date as more and more Raions are available to the estimation.

events there is a decline of the average treatment effect, while, in the medium-term, we note that, although there was a small rebound, the negative gap still holds and a declining trend is still recognizable.[27]

5. Additional analyses

The nature of the phenomenon under study requires a further assessment of the average treatment effect under the dimension of both time and space. Indeed, the latter baseline results rely on several assumptions: a) treatment intensity is homogeneous over Raions and over time, b) the whole Raion is homogeneously impacted by the conflict, and c) the presence of spatial spillovers between contiguous Raions is negligible. In the following sub-sections we relax each of them, showing on the one side the robustness of our main results and on the other side possible extension to our findings.

5.1. Temporal and spatial variation in attacks

The first assumption we relax is the treatment homogeneity over time and space. Indeed, as reported in Figure 1, the intensity of the conflict greatly varies across Raions, suggesting the presence of heterogenous treatment effects deepening on heterogenous treatment intensities (i.e., number of military events). Furthermore, as reported in Appendix A11, number of events greatly varies also on a temporal dimension, with about 15,000 events in March 2022, followed by a declining trend to about 5,000 events per month in 2023. These two evidences suggest that we should look in detail to both dimensions of treatment heterogeneity.

As first preliminary evidence, we estimate the following regression in eq. (3) which takes the form of a *continuous treatment* design.

$$Y_{it} = \alpha_i + \beta\, Conflict_{it} + \delta\, Conflict_{it} \times\ asinh(Events_{it}) + \gamma\, X_{it} + \tau_t + \varepsilon_{it} \qquad (3)$$

Here we are interested in the coefficient estimate of δ representing the additional average marginal effect per a percentage increase in the number of military events. In this sense, δ represents the differential effect of heterogenous treatment *dosages* varying over time and Raions. Estimates in Table 7 report in the most complete specification (M2.3) that, while the average decrease of night-light intensity is around -3% in treated Raions following the first military event, night-light intensity is also significantly determined by the number of military events.[28] In fact, we estimate that doubling the number of events, additionally decreases night-light intensity by around 3.5%.[29]

[27] In Appendixes A8, A9, A10 we provide the event study plots using as dependent variables $DensLight_{it}$, $MedLight_{it}$ and $asinh\ MedLight_{it}$ respectively. In all cases we confirm the pattern evidenced in Figure 3. However, it is worth to mention that canonical OLS TWFE estimates when $DensLight_{it}$ is the dependent variable show a systematically negative and significant estimates of all leads. By contrast, $MedLight_{it}$ (either in linear or *asinh* transformed) shows a strongly robust absence of pre-treatment differences in trends, particularly when Callaway and Sant'Anna (2021) is used as estimator.

[28] In Appendix A12 we show similar results using $MedLight_{it}$ as dependent variable.

[29] Elasticity computed as $2^{\delta} - 1 = 2^{-0.052} - 1 = -0.035$.

Table 7: Baseline continuous treatment design.

	$\mathbf{y} = DensLight_{it}$			$\mathbf{y} = \boldsymbol{asinh}\ DensLight_{it}$		
	M1.1	**M1.2**	**M1.3**	**M2.1**	**M2.2**	**M2.3**
$Conflict_{it}$	0.015	-0.801*	-0.179	-0.025	-0.046**	-0.034*
	(0.359)	(0.479)	(0.256)	(0.020)	(0.018)	(0.018)
$Conflict_{it} \times$ *asinh* $Events_{it}$	-0.902***	-0.855***	-0.515***	-0.071***	-0.056***	-0.052***
	(0.348)	(0.290)	(0.144)	(0.013)	(0.010)	(0.010)
Constant	22637.654***	7.355***	22680.759***	2897.916***	2.095***	2922.567***
	(8334.314)	(0.104)	(8347.190)	(328.452)	(0.004)	(327.916)
Controls *weather-related*	Yes	No	Yes	Yes	No	Yes
Controls *conflict-related*	No	Yes	Yes	No	Yes	Yes
Raion FE	Yes	Yes	Yes	Yes	Yes	Yes
Time FE	Yes	Yes	Yes	Yes	Yes	Yes
N	31,144	32,164	31,144	31,144	32,164	31,144
R2	0.726	0.798	0.728	0.842	0.897	0.842
Within R2	0.043	0.030	0.048	0.080	0.074	0.083

Notes: a) *** p<0.01, ** p<0.05, * p<0.10, b) clustered standard errors at the Raion level in parentheses; c) Controls *weather-related* contains: $Temperature_{it}$ (in linear and quadratic terms), $Rainfalls_{it}$ and $WindSpeed_{it}$; d) Controls *conflict-related* contains: FRP_{it} and $AntiAirDefence_{it}$.

However, in this specific empirical setting, the nature of heterogenous treatment *dosages* requires further examination. A Raion can, indeed, receive multiple military events all concentrated in a month, or over multiple (subsequent or not) periods. This raises further considerations on the corresponding estimated average treatment effect, where we have to disentangle the immediate effect of a single military event, from its long-lasting impact and from the cumulative effects of repeated treatment over multiple (subsequent) periods.

Appendixes A13 and A14 provide descriptive evidence on our case. Within the 338 treated Raions, about 70% received 1 to 5 military events in the first month of the conflict,[30] while a minor subset (about 1%) received more than 100 attacks in the first month. Looking at the patterns of treatment intensity, we also note that in 41% of the cases (Raion-month observations in treated Raions, following the first treatment date), there is not treatment intensity variation from one month to the other, while, in 32% of cases and 27% we see, respectively, decreases and increases in treatments with respect to the previous month. Appendix A14 shows descriptive statistics on treatment paths. About 19% of treated Raions have been continuously treated from February 2022 to August 2023, counting on average about 113 military events per month. These Raions accounted for 86% of total military events in our data. On the opposite side, about 30% of Raions never saw two consecutive periods with military events greater than 0. What emerges is that our empirical setting is clearly characterized by large heterogeneity in treatment patterns across the various Raions.

Applied economics research suggests that a possible way to disentangle the presence of cumulative treatment effects is to estimate a canonical event-study like analysis using a distributed lag model with leads and lags indicating past and future treatments (Fenton and Koenig, 2025; Schmidheiny and Siegloch, 2019).[31] In this study we conduct a similar exer-

[30] That is, in econometric terms, at the treatment allocation date.

[31] In their paper, Fenton and Koenig (2025) estimate the effect of TV rollout in the US on retirement

cise, yet building on the recent methodological advancements proposed by De Chaisemartin and d'Haultfoeuille (2024). In their paper, De Chaisemartin and d'Haultfoeuille (2024) propose a difference-in-differences estimator suitable for cases in which the treatment may be staggered, non-binary, not absorbing and where, more importantly, lagged treatments may affect future outcomes. In this sense, this estimator is an extension of Callaway and Sant'Anna (2021) and Borusyak et al. (2024), previously applied to estimate static and dynamic average treatment effect on treated Raions, given that they assume a binary and absorbing treatment. De Chaisemartin and d'Haultfoeuille (2024), by construction, can be used, instead, with a continuos treatment that can increase or decrease multiple times and where the current and lagged treatments may have heterogeneous effects over space and/or over time, resembling to a situation closely adhering to ours where multiple military events overlap each other.

In Figure 4 we report the estimates of the average marginal effect of a percentage increase in $Events_{it}$ on night-light intensity. This is a *normalized* event study estimate, where the time axis is aligned on the period before last treatment change (marked with 0 and a vertical dashed reference line). The term *normalized* means that we use *normalized weights* per each time lead. In other words, event-study estimate at T = +1 (period in which treatment changes, i.e., there are new military events) is the average marginal effect of these contemporaneous military events on night-light intensity. The second normalized effect (at T = +2) is the weighted average (with approximately similar weights) of the effects of contemporaneous events and of the first lag of of events on night-light intensity (those allocated in the previous period), and so on. Hence, the interpretation of Figure 4 is notably different from those of Figure 3. While *TWFE OLS*, Borusyak et al. (2024) and Callaway and Sant'Anna (2021) (in Figure 3) provide estimates of the average treatment effect at l periods after the *first* treatment change (i.e., treatment allocation date),[32] De Chaisemartin and d'Haultfoeuille (2024) (in Figure 4) allows to distinguish between short-run and long run effects of the single military event, even in presence of multiple, repeated, treatments.[33]

Figure 4 provides several intuitions. First, as in line with Figure 3, prior to treatment change, we do not observe significant deviations from zero, meaning that we can plausibly confirm the validity of the parallel trend assumption with this alternative estimation strategy. Second, we show a heterogenous pattern depending on the temporal lags l we

decision. Their case is similar to our as their treatment is represented by the number of TV stations in an area at a given period. Hence, more importantly, their setting is characterized by a repeating treatment, where the effect of future openings of TV stations overlaps with the effect arising from past openings, just like our case where future military events overlap with past ones. To estimate the dynamics of treatment effect, they show the estimates using an event study approach with distributed lags, which, however, may not fully disentangle the immediate and cumulative effects of a treatment dosage change.

[32] Note that l indicates the number of periods after the treatment change.

[33] For the sake of comparison, in Appendix A15 we report estimates of the canonical event study (i.e., with non-normalized weights) using De Chaisemartin and d'Haultfoeuille (2024), hence closely resembling to the methods of Callaway and Sant'Anna (2021) and Borusyak et al. (2024). Results are rather similar.

Figure 4: Average marginal effect of $Events_{it}$ by temporal lag.

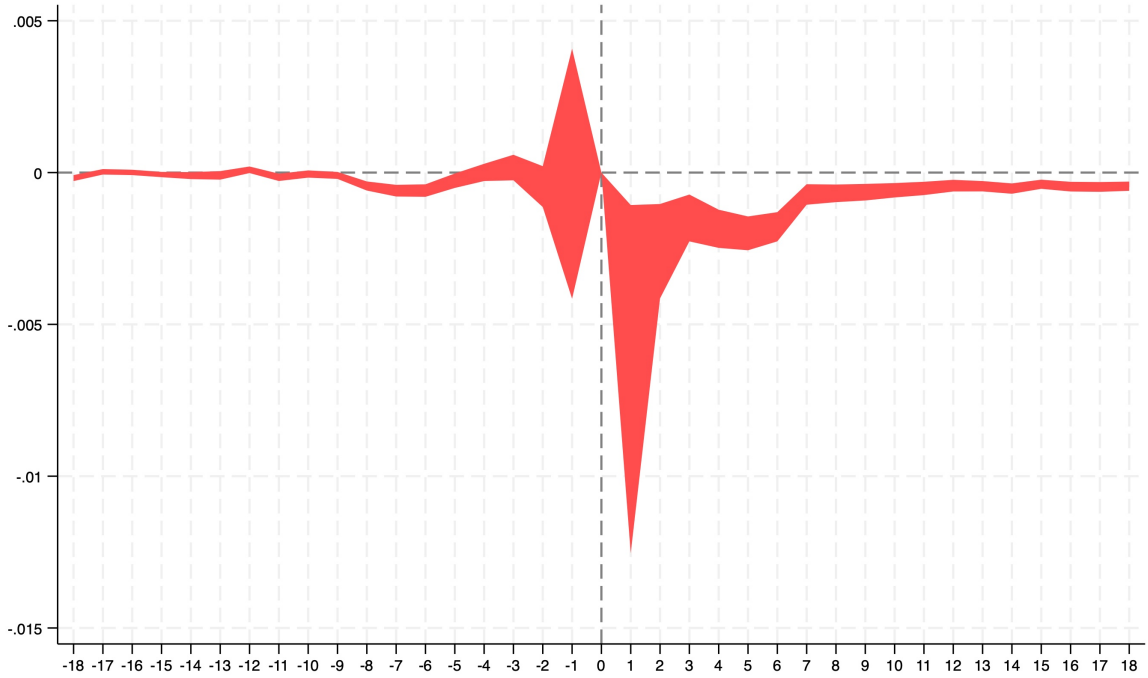

Notes: a) 95% confidence interval based on clustered robust standard errors at the Raion level is shown; b) the vertical line (dash line on 0) refers to one period (i.e., month) before the treatment change; c) estimated using De Chaisemartin and d'Haultfoeuille (2024) with *normalized weights*; d) the graph is estimates using the accompanying Stata package *did_multiplegt_dyn* released by De Chaisemartin and d'Haultfoeuille (2024); e) the estimator allows placebo (i.e., pre-trends) estimates only on a symmetric window, meaning that we can observe pre-trends only up to 18 periods before treatment change; f) dependent variable = $asinh\ DensLight_{it}$.

observe. In general, we note that normalized event-study estimates are getting closer to zero with increasing values of l. This evidence indicates that at the moment of treatment change (i.e., $l = +1$) a strong and significant negative marginal effect emerges, meaning that immediately following the event night-light intensity remarkably decreases. Furthermore, the *direct* effects of military events are largely, though not entirely, absorbed within six to seven months, implying that lagged military events exert a smaller influence on night-light intensity than contemporaneous ones (De Chaisemartin and d'Haultfoeuille, 2024). Coherently, if we jointly analyse Figures 3 and 4 we can understand the dynamic of the events: the negative gap evidenced in canonical event study estimates (which does not seem to recover in the 18 months we observe) is, in fact, consequence of multiple military events allocated to the same Raion at staged periods (as in line with the descriptive

evidence in Appendix A14).[34]

5.2. Within Raion average treatment effect

A special feature of night-light data is that they come at a spatially granular level that we later aggregate at the Raion level.[35] Compared to other traditional socio-economic variables (e.g., GRP, employement, etc.) – which comes at the regional level, without any possibility to disentangle local heterogeneity – this means that with night-lights, even though we analyse data at the regional level, we still can provide information at a higher spatial resolution.

Our previous estimates, whether they are referring to static, dynamic or marginal average treatment effects, estimated a negative shift of the mean night-light intensity produced by a given Raion following military events. Such a shift, however, can come in a variety of ways. For instance, the whole distribution of night-lights within Raions can shift to the left, keeping its internal variation constant: this would mean that the conflict had an homogeneous impact on all areas within the Raion, whether they produce high or low night-light intensity. More likely, the significant decrease in the mean value could also be attributed to a *shrinkage* of the distribution (i.e., a decline of the standard deviation) due to the fact that we can expect a more proportional decline of brighter areas (e.g., more productive) compared to less bright ones. In other words, we expect military events to have been selectively allocated to productive areas within a Raion, hence reducing night-light intensity at the brightest parts of the region.

To provide evidence on this, we designed the following exercise. We estimated Equation 1 using different dependent variables, namely $IQRLight_{it}$, $p25Light_{it}$ and $p75Light_{it}$. The first is the interquartile range of the pixel-level within Raion distribution, representing the distance between brightest and darker parts of the Raion. The second and the third variables represent the night-light intensity at the bottom/top part of the distribution of night-light intensity.

Table 8 reports the estimation results[36] using canonical TWFE OLS estimator.[37] We find robust evidence on the fact that following the first military event, the distance between the first and third quartile of the within Raion night-light distribution significantly decreased. In other words, night-light intensity at brightest areas came closer to night-light intensity at darkest areas. In fact, looking at separate estimates, we see that the average treatment effect on the $p75Light_{it}$ is nearly three times larger than the average effect on $p25Light_{it}$.

[34] To complement this estimates, in Appendix A16 we show the weights employed by De Chaisemartin and d'Haultfoeuille (2024) to retrieve the estimates in Figure 4; in Appendix A17 we show the same estimates using $DensLight_{it}$ (in levels), $MedLight_{it}$ (in levels) and $asinh\ MedLight_{it}$.

[35] Recall from Section 3 that original night-light data are at the pixel level, a raster of $0.5km \times 0.5km$.

[36] Note that we tested the dependent variables in both linear and *asinh*-transformed versions.

[37] In Appendix A18 we also show the results using the estimators of Borusyak et al. (2024) and Callaway and Sant'Anna (2021), with rather similar results, with a larger evidenced gap between the 25th percentile and the 75th one (i.e., the average treatment effect on the right part of the distribution is nearly 5 times larger than those on the left part when these estimators are used).

Table 8: Within Raion average treatment effect.

Dependent variable	$IQRLight_{it}$	*asinh* $IQRLight_{it}$	$p25Light_{it}$	*asinh* $p25Light_{it}$	$p75Light_{it}$	*asinh* $p75Light_{it}$
	M1.1	**M1.2**	**M2.1**	**M2.2**	**M3.1**	**M3.2**
$Conflict_{it}$	-0.068**	-0.031***	-0.016*	-0.013***	-0.083**	-0.036***
	(0.034)	(0.009)	(0.008)	(0.005)	(0.042)	(0.009)
asinh $Temperature_{it}$	-766.976**	-181.256***	-238.901	-105.761**	-1005.878**	-202.803***
	(347.586)	(60.249)	(159.654)	(43.682)	(490.856)	(59.082)
asinh $Temperature_{it}^2$	60.228**	14.328***	18.557	8.130**	78.785**	15.854***
	(27.277)	(4.740)	(12.522)	(3.433)	(38.508)	(4.643)
asinh $Rainfalls_{it}$	0.018***	0.011***	-0.004*	-0.006***	0.013**	0.004***
	(0.004)	(0.001)	(0.003)	(0.001)	(0.006)	(0.001)
asinh $WindSpeed_{it}$	-0.035	-0.025**	-0.013	-0.015**	-0.048	-0.039***
	(0.031)	(0.010)	(0.010)	(0.007)	(0.037)	(0.010)
FRP_{it}	0.002**	0.000***	0.000	-0.000**	0.002*	-0.000
	(0.001)	(0.000)	(0.000)	(0.000)	(0.001)	(0.000)
asinh $AntiAirDefence_{it}$	-0.210*	-0.083***	-0.059	-0.026	-0.269*	-0.080***
	(0.115)	(0.028)	(0.047)	(0.017)	(0.161)	(0.027)
Constant	2,441.912**	573.411***	769.159	344.150**	3,211.070**	649.083***
	(1107.265)	(191.447)	(508.845)	(138.945)	(1564.131)	(187.949)
Raion FE	Yes	Yes	Yes	Yes	Yes	Yes
Time FE	Yes	Yes	Yes	Yes	Yes	Yes
N	31,144	31,144	31,144	31,144	31,144	31,144
R2	0.699	0.853	0.666	0.789	0.695	0.859
Within R2	0.026	0.073	0.018	0.023	0.026	0.065

Notes: a) *** p<0.01, ** p<0.05, * p<0.10, b) clustered standard errors at the Raion level in parentheses; c) $IQRLight_{it}$ is the *interquartile range* of the pixel-level distribution within Raion i of night-light at month t; d) $p25Light_{it}$ is the *first quartile* of the pixel-level distribution within Raion i of night-light at month t; e) $p75Light_{it}$ is the *first quartile* of the pixel-level distribution within Raion i of night-light at month t; f) estimates are done using canonical TWFE OLS estimator - in Appendix A18 we resort to the estimators of Borusyak et al. (2024) and Callaway and Sant'Anna (2021).

This evidence provides information on the nature of military events and their *selective* effect. The fact that brightest areas have been more affected than darker areas means, reasonably, that a) most likely attacks have been selectively allocated to productive areas within a Raions, and b) the (negative) effect is hence largely concentrated on this top right part of the distribution. Furthermore, on a different note, the results and the insights in Table 8 explain the difference in magnitude of the average treatment effect when $MedLight_{it}$ is used as dependent variable instead of $DensLight_{it}$ (our preferred specification). In fact, the former indicator (i.e., $MedLight_{it}$), being structurally less sensible to outliers truncation, has shown a relatively less pronounced decline compared to $DensLight_{it}$, that is, in essence, a Raion-average value.

Finally, partially confirming this hypothesis, it is worth to see the estimated elasticity of the different dependent variables to the number of anti-air defence events. We estimate, indeed, that while the third quartile of night-light intensity is significantly – and negatively – correlated with the regional number of such events, the first quartile is not. This is in line with the nature of such events, which artificially turn off lights in a preventive manner, likely in urban centres where most of the population lives and where night-lights are expected to be higher.

5.3. Spatial controls

So far, in previous analyses, Raions have been considered as separate entities, neglecting the spatial feature of the data. In this section we explore the spatial structure of Raions to

Table 9: Average treatment effect estimates using spatial controls

	y = ***asinh*** $DensLight_{it}$					
	M1	**M2**	**M3**	**M4**	**M5**	**M6**
$Conflict_{it}$	-0.088***	-0.031*	-0.083***	-0.089***	-0.091***	-0.067***
	(0.018)	(0.016)	(0.019)	(0.018)	(0.018)	(0.016)
asinh mean FC $DensLight_{it}$		0.760***				0.785***
		(0.032)				(0.032)
asinh sum FC $Events_{it}$			-0.003			0.028***
			(0.006)			(0.005)
asinh $distZaporizhzhia_i \times PostFebruary2022_t$				-0.023		0.016
				(0.096)		(0.089)
$BorderRussianControl_i \times PostFebruary2022_t$					0.164***	-0.037
					(0.050)	(0.045)
Constant	2,902.423***	515.843*	2,913.140***	2,897.758***	2,886.956***	349.465
	(329.005)	(262.585)	(326.011)	(319.911)	(328.838)	(254.703)
Controls *weather-related*	Yes	Yes	Yes	Yes	Yes	Yes
Controls *conflict-related*	Yes	Yes	Yes	Yes	Yes	Yes
Raion FE	Yes	Yes	Yes	Yes	Yes	Yes
Time FE	Yes	Yes	Yes	Yes	Yes	Yes
N	31,144	31,144	31,144	31,144	31,144	31,144
R2	0.840	0.908	0.840	0.840	0.841	0.910
Within R2	0.071	0.465	0.071	0.071	0.073	0.476

Notes: a) *** p<0.01, ** p<0.05, * p<0.1; b) clustered standard errors at the Raion level in parentheses; c) FC = in first contiguous Raions, defined by *Queen Contiguity* logic; d) Controls *weather-related* contains: $Temperature_{it}$ (in linear and quadratic terms), $Rainfalls_{it}$ and $WindSpeed_{it}$; e) Controls *conflict-related* contains: FRP_{it} and $AntiAirDefence_{it}$; f) the model is estimated through OLS TWFE, in Appendix A21 we report estimates with BJS and CS.

further control for potential spatially-related confounds that are likely to exert a significant impact on the observed night-light intensity.

Table 9 reports the results where several controls have been included.[38,39] It is worth to note that in all cases the corresponding average treatment effect associated to $Conflict_{it}$ always remains negative and statistically significant and β varies in the range between -0.031 to -0.091. We now describe the intuitions behind each new control variables.

Models M2 controls for the spatial lag of the dependent variable (*asinh mean FC* $DensLight_{it}$), that is defined as the mean night-light density at period t of Raions that are first contiguous to Raion i. The corresponding coefficient is positive and strongly significant, meaning that the dependent variable under analysis is characterized by a strong degree of (positive) spatial autocorrelation: it is likely to find a higher night-light intensity closer to Raions with higher night-light intensity, controls coeteris paribus. This evidence demonstrate that our data are characterized by clusters of high and low nightlight intensity, suggesting that the Raion level can be even too narrow to observe such a phenomenon.

Model M3 controls for a spatial lag of the main explanatory variables, as the *asinh* of the

[38] For the sake of clarity, we show, as a benchmark the baseline model M1, that is equivalent to model M2.3 in Table 5

[39] Table 8 uses OLS TWFE to estimate the average treatment effect on *asinh* $DensLight_{it}$. In Appendix A19, A20 and A21 we report the same specifications using: a) $DensLight_{it}$, $MedLight_{it}$ and *asinh* $MedLight_{it}$ as dependent variables, and b) BJS and CS as estimators.

number of military events in first contiguous Raions ($asinh\ sum\ FC\ Events_{it}$) is included as regressor. This variable is not significantly correlated with the dependent variable, meaning that we do not observe spatial spillovers following military attacks in a given Raion. In other words, the negative effects following a military event (evidenced in both Tables 5 and 6) is primarily observed in the corresponding Raion, while no significant effects in nearby locations are observed, controls coeteris paribus.

Model M4 includes a control related to the consequences of war events that are capable to trigger confounds that will likely have an impact on the observed night-light. In fact, we add a control on the distance from the nuclear power plant of Zaporizhzhia. In Ukraine there are 4 plants: Zaporizhzhia, Rivne, Khmelnitsky and Yuzhnoukrainsk. These account for more than 50% of the country energetic mix, hence resulting in an important source of energy for the local community. Remarkably, the nuclear plant of Zaporizhzhia received multiple military attacks, and, during the conflict, it frequently stopped its energetic production and passed under the Russian control. To this extent, being closer or further from Zaporizhzhia may represent a crucial confound: the closer the Raion, the higher the likelihood to source energy from the *attacked* plant, the higher the likelihood to incur in blackouts or energy stops due to *infrastructural* damages. To account for this hypothesis, we control for the *asinh* of the distance of each Raion to the Zaporizhzhia nuclear plant, multiplied by a dummy indicating the conflict period (from February 2022 onwards). Regression result shows that this confound is not significantly determining variations in observed night-light density.

On a different note, in Model M5, we control for border effects. Particularly, we also control for the fact that a Raion is neighbouring to Russian controlled ones (i.e., it shares at least one common border with one of the excluded Raions in the Oblasts of Crimea, Lugansk and Sebastopol City). We find that, in the Raions close to Russian-controlled areas, night-light intensity after the conflict's onset followed a different trend than in the rest of Ukraine – remaining stable or even rising – indicating a likely increase in activity plausibly linked to military operations.

Finally, Model M6 report full models with all spatial control jointly included as regressors. The regions bordering Russian-controlled areas experienced intense and widespread fighting. Accordingly, the results from Model M6 confirm the (relative) increase in luminosity in these areas after February 2022, as suggested by Model M5, while the average treatment effects for the other variables remain largely unchanged.

6. From night-lights to economic impact

At this stage of the study, various strands of literature motivate us to extend our analysis to examine how our precise measures of changes in night-lights – *directly* and *locally* attributable to shocks (in our case, specific military attacks) – can be used to predict the socio-economic consequences of these events.

On the one hand, we can draw on Henderson et al. (2012) and the subsequent literature that directly estimate the elasticity of economic output variables (e.g., GDP) with respect to

Figure 5: Estimated heterogenous night-light density drop (continuous treatment design)

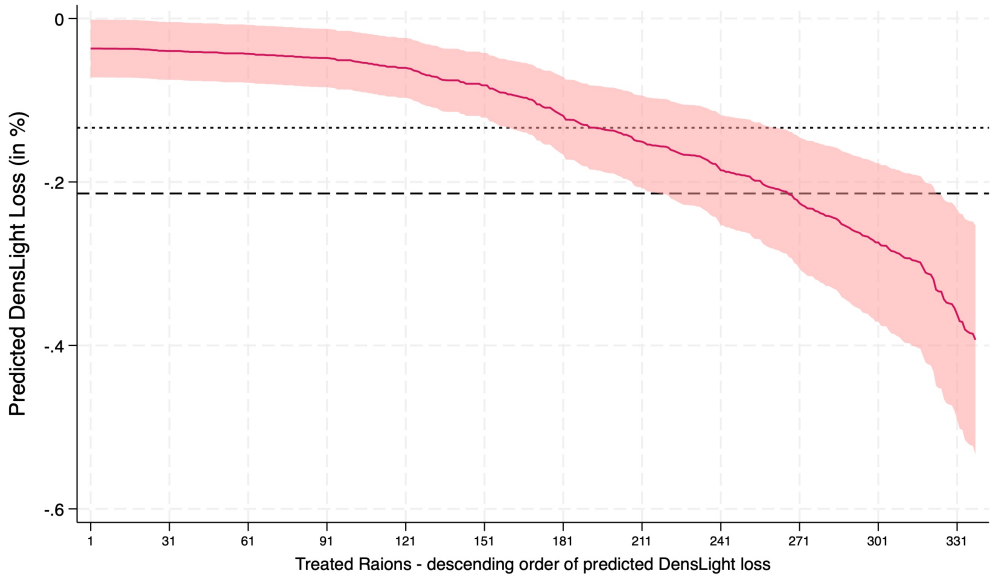

Notes: a) the red line is the fitted night-light density percentage drop according to estimated regression coefficients in model M2.3. of Table 7 using the average number of military events in the given Raion after the first event; b) 95% confidence interval based on estimates clustered standard errors is shown; c) Raions are ranked in descending order of fitted night-light drop; d) short-dashed line represent simple average night-light drop (≈ -13%); e) dashed line represented weighted average night-light drop with weights based on Raions' population (≈ -21%).

changes in night-light intensity. The literature discussed in Section 1, by contrast, examines the long-term persistence of the effects of prolonged warfare and employs indicators of military activity intensity (e.g., bombing intensity in specific areas) for this purpose. This line of research could benefit from metrics that translate the severity of shocks into short-term actual outcomes, such as economic losses and reductions in human activity. Therefore, in this section, we examine how precisely this decline can be used to assess the corresponding economic impact, as well as the limitations of this approach.

There are multiple ways to estimate the average night-light drop for treated Raions. First, we have introduced in Section 4.2 a measure of the static average treatment effect on the treated, estimated with a canonical OLS TWFE. Then, we have introduced estimators suitable for *staggered* designs in Section 4.3, for removing the influence of forbidden comparisons. These two estimates measure the decline in night-light intensity in treated Raions compared to counterfactual outcomes (i.e., the not-treated Raions), averaging over all Raions and all periods after the first attack. Finally, we have taken into account Raion heterogenous drops, exploiting the continuos treatment strategy reported in Section 5.1 and the heterogeneity in the number of events per each Raion.

The inference derived from these various estimates yields specific predictions of night-light

variations at the scale of each treated Raion. The Raion variations corresponding to continuous treatment estimates are reported in Figure 5: the average Raion (i.e., one with an average number of attacks) experienced an expected decline in night-light intensity of -13.4% (represented by the dotted horizontal line), with estimates reaching approximately -40% in the case of Raions subjected to exceptionally high levels of attack.

Individual Raion-level predictions can then be aggregated at the national level, either as a simple average or weighted by each Raion's population.[40,41] The population-weighted expected decline in night-lights, according to the continuous treatment estimates, increases to -21.4% (shown as the dashed horizontal line in Figure 5).

Table 10 presents, in the first column, the average night-light losses of treated regions (i.e., those that experienced at least one military attack between February 2022 and August 2023), along with their standard errors, relative to non-treated regions. First, we observe that our estimates vary considerably, ranging from -8.8% to -17.8% in the unweighted cases and from -18.2% to -64.9% in the weighted ones.
This evidence first indicates that our unweighted estimates are highly conservative – reflecting the fact that military attacks were (unsurprisingly) concentrated in the most densely populated and likely most economically productive Raions. Second, as we report in 4.3, the evidence highlights that OLS TWFE predictions substantially underestimate night-light losses due to the inclusion of forbidden comparisons. Third, a significant share of the total estimated night-light losses can be attributed to the cumulative impact of multiple shocks, which were disproportionately concentrated in more densely populated Raions. This is reflected in the substantial gap between the BJS and CS estimates and the continuous treatment estimates, the latter capturing the effect of individual shocks.

We can now undertake the task of translating the expected night-light losses, using the results reported in the first column of Table 10, into corresponding GDP variations. To do so, we draw on elasticity estimates from the literature – specifically, the values reported in Henderson et al. (2012, Table 3, p. 1015), where the elasticity between GDP and night-lights is estimated to range from 0.180 to 0.320. The second and third columns of Table 10 convert night-light losses into corresponding GDP losses, using the lower and upper bounds of the elasticity estimated by Henderson et al., respectively. The more realistic economic estimates of the impact of military events on the whole Ukrainian

[40] In this sense, we make the fair assumption that the expected reduction in the anthropogenic activity proxied by night-light intensity following a military event is more important where the more population lives in that area. Similarly, Yamada and Yamada (2021) construct an indicator of the short-term severity of bombing campaigns during the Vietnam War by adjusting bombing data with historical population density to better capture expected economic losses.

[41] In Appendix A22 and 23 we show the output of weighted regression model in the static and dynamic specifications. It is worth to mention that weights, giving more importance to Raions with higher population, provide a significantly larger estimate of the average treatment effect. Nonetheless, the event study plots reported in Appendix A23 suggests that even with weights, trends before the first military event in treated and control Raions are parallel, with some leads that are significantly different from zero, yet located either above of below it.

Table 10: Estimated average GDP loss.

Weights	Estimation Method	Avg. Expected Night-light Loss	Avg. Expected GDP Loss - LB	Avg. Expected GDP Loss - UB
Unweighted	OLS TWFE	-0.088	-0.016	-0.028
		(0.018)	(0.004)	(0.006)
	Borusyak et al. (2024)	-0.171	-0.031	-0.055
		(0.029)	(0.008)	(0.011)
	Callaway and Sant'Anna (2021)	-0.178	-0.032	-0.057
		(0.028)	(0.008)	(0.011)
	Continuous Treatment	-0.134	-0.024	-0.043
		(0.005)	(0.005)	(0.005)
Weighted	OLS TWFE	-0.182	-0.033	-0.058
		(0.042)	(0.010)	(0.015)
	Borusyak et al. (2024)	-0.598	-0.108	-0.191
		(0.112)	(0.029)	(0.042)
	Callaway and Sant'Anna (2021)	-0.649	-0.117	-0.208
		(0.135)	(0.034)	(0.050)
	Continuous Treatment	-0.214	-0.039	-0.068
		(0.006)	(0.008)	(0.008)

Notes: a) standard errors in parentheses; b) Expected GDP losses computed using estimates of Henderson et al. (2012) in its Table 3; c) LB stands for *Lower Bound* and uses an estimated elasticity of GDP growth to night-light variations of 0.180 (s.e. = 0.036) (i.e., column 2 in Henderson et al., 2012); d) UB stands for *Upper Bound* and uses an estimated elasticity of GDP growth to night-light variations of 0.320 (s.e. = 0.037) (i.e., column 4 in Henderson et al., 2012).

economy are given by the weighted staggered estimates, between -10.8% and -20.8%, which represent the combined effects of repeated and targeted attacks across the entire Ukrainian territory. Official estimates report that Ukraine's real GDP in 2022 harshly fell by 29.2% with respect to 2021.[42]

Our estimate accounts for only about half of the official figures; however, it is important to emphasize the reasons why the two measures are only partially comparable, as well as the inherent limitations of this exercise, which seeks to translate changes in luminosity into changes in economic output.

First, Henderson et al. (2012) estimate their elasticity under normal conditions of economic activity, not in situations of severe disruption; the night-lights–GDP elasticity corresponding to such shocks should be specifically estimated and may differ substantially.[43]

Second, our analysis focuses solely on the *direct* effects of military events on the *treated* regions. Consequently, the estimates presented pertain only to a subset of Ukrainian regions.[44] Naturally, a significant share of the total loss in value is likely due to *indirect* effects impacting the entire country – such as reduced competitiveness, declines in inter-

[42] Sourced from the Ukrainian Government portal at https://www.kmu.gov.ua/en/news/minekonomiky-vvp-za-pidsumkom-2022-roku-vpav-na-292

[43] Yamada and Yamada (2021) argue that night-light intensity is a superior measure for assessing the immediate impacts of conflict, as it more precisely reflects the destruction of housing, infrastructure, and production facilities compared to other economic indicators.

[44] Raions that were never attacked account for roughly 20% of the national GDP (see again Table 3). However, in the staggered estimates, Raions classified as 'not yet attacked' also contribute to the set of non-treated observations.

national trade, etc. – which cannot reasonably be expected to be reflected in night-light losses. In other words, during structural shocks such as armed conflicts, economic activity should respond much more sharply to changes in night-light intensity than under the normal economic conditions assumed in previous models.
Finally, our estimate is short-term, whereas the estimates in Table 10 implicitly assume that night-time light losses following attacks are persistent. In contrast, our continuous treatment approach indicates that the effects of individual attacks tend to dissipate over the medium term – so much so that repeated attacks on specific Raions are required to produce lasting impacts. In this sense, our GDP loss estimates may even overstate the actual effects.

7. Conclusion

This paper provides and empirical examination on the impact of russo-ukrainian conflict onto Ukraine's economic activity. Given the limitation of traditional economic measures (e.g., GDP, GVA), that are either not yet available, nor frequently updated or promptly released, we propose – and test – satellite imagery, namely night-light luminosity, as useful source.

Following a precise methodology to control for the presence of confounds strictly related with the nature of our data (e.g., temperature, fireplaces, anti-air attack strategies), we test these data into a causal setting exploiting a difference-in-differences methodology. We find significant and very robust results. On average, using a prudential estimate we find that following the first military event, attacked Raions saw a decline of average night-light luminosity around -16.0%.[45] This result is consistent across the different estimators, required for the staggered nature of our difference-in-differences design (Borusyak et al., 2024; Callaway and Sant'Anna, 2021). Building on baseline estimates, we also provide several variations. First, we show the temporal dynamics of the average treatment effect using an event study design, showing that recovery has not yet been reached. Second, we complement such an event study applying the estimator of De Chaisemartin and d'Haultfoeuille (2024), which allows us to disentangle short- and medium/long-run effects of single military events in presence of repeated and cumulative effects. We show that the marginal effect of an event is large in the immediate surroundings of the event, and tend to vanish in 6-7 months. This suggest that the missing recovery is consequence of multiple overlapping events allocated at staged times. Third, we also show, by the means of the specific characteristics of night-lights, that the major effects are recorded in the brightest (i.e., most productive) parts of the Raion. Finally, we also provide an economic assessment, showing that, based on the estimates of Henderson et al. (2012), expected GDP loss can be estimated between -10% and -20% (compared to a -29.2% official estimate), suggesting that GDP-nightlights elasticity is way larger in presence of a structural shock such as military conflicts.

[45] See Section 4.3 to retrieve this estimate.

Overall, this paper offers to economic researchers new possibilities when evaluating the impact of (exogenous) shocks. Next to other satellite imagery – e.g., vehicles flow as in Go et al. (2022) – night-lights offer a valuable data source thanks to the special features they have, the strong correlation with traditional economic accounts (Henderson et al., 2012) and the robustness in causal inference settings to alternative (and newest) estimators.

References

Azariadis, C. and Drazen, A. (1990). Threshold externalities in economic development. *The Quarterly Journal of Economics*, 105(2):501–526.

Berger, T., Chen, C., and Frey, C. B. (2018). Drivers of disruption? estimating the uber effect. *European Economic Review*, 110:197–210.

Bickenbach, F., Bode, E., Nunnenkamp, P., and Söder, M. (2016). Night lights and regional GDP. *Review of World Economics*, 152(2):425–447.

Borusyak, K., Jaravel, X., and Spiess, J. (2024). Revisiting event-study designs: robust and efficient estimation. *Review of Economic Studies*, 91(6):3253–3285.

Bowles, S., Durlauf, S. N., and Hoff, K. (2011). *Poverty traps*. Princeton University Press.

Braghieri, L., Levy, R., and Makarin, A. (2022). Social media and mental health. *American Economic Review*, 112(11):3660–3693.

Brakman, S., Garretsen, H., and Schramm, M. (2004). The strategic bombing of German cities during World War II and its impact on city growth. *Journal of Economic Geography*, 4(2):201–218.

Burtch, G., Carnahan, S., and Greenwood, B. N. (2018). Can you gig it? an empirical examination of the gig economy and entrepreneurial activity. *Management science*, 64(12):5497–5520.

Callaway, B. and Sant'Anna, P. H. (2021). Difference-in-differences with multiple time periods. *Journal of Econometrics*, 225(2):200–230.

Davis, D. R. and Weinstein, D. E. (2002). Bones, bombs, and break points: the geography of economic activity. *American Economic Review*, 92(5):1269–1289.

De Chaisemartin, C. and d'Haultfoeuille, X. (2024). Difference-in-differences estimators of intertemporal treatment effects. *Review of Economics and Statistics*, pages 1–45.

Fenton, G. and Koenig, F. (2025). Labor supply and entertainment innovations: Evidence from the US TV rollout. *American Economic Journal: Applied Economics*, 17(4):1–28.

Freyaldenhoven, S., Hansen, C., Pérez, J. P., and Shapiro, J. M. (2021). Visualization, identification, and estimation in the linear panel event-study design. Technical Report n. w29170, National Bureau of Economic Research.

Gibson, J., Olivia, S., and Boe-Gibson, G. (2020). Night lights in economics: sources and uses. *Journal of Economic Surveys*, 34(5):955–980.

Giovannetti, G. and Perra, E. (2020). Syria in the dark: estimating the economic consequences of the civil war. Technical Report n. 29, EMNES Working Paper.

Go, E., Nakajima, K., Sawada, Y., and Taniguchi, K. (2022). On the use of satellite-based vehicle flows data to assess local economic activity: the case of Philippine cities. Technical Report n. 652, ADB Economics Working Paper Series.

Goodman-Bacon, A. (2021). Difference-in-differences with variation in treatment timing. *Journal of Econometrics*, 225(2):254–277.

Guo, S. (2020). The legacy effect of unexploded bombs on educational attainment in Laos. *Journal of Development Economics*, 147:102527.

Hale, T., Angrist, N., Goldszmidt, R., Kira, B., Petherick, A., Phillips, T., Webster, S., Cameron-Blake, E., Hallas, L., Majumdar, S., et al. (2021). A global panel database of pandemic policies (Oxford COVID-19 Government Response Tracker). *Nature Human Behaviour*, 5(4):529–538.

Harari, M. (2020). Cities in bad shape: urban geometry in India. *American Economic Review*, 110(8):2377–2421.

Henderson, J. V., Squires, T., Storeygard, A., and Weil, D. (2017). The global distribution of economic activity: nature, history, and the role of trade. *The Quarterly Journal of Economics*, 133(1):357–406.

Henderson, J. V., Storeygard, A., and Weil, D. N. (2012). Measuring economic growth from outer space. *American Economic Review*, 102(2):994–1028.

Koenig, F. (2023). Technical change and superstar effects: Evidence from the rollout of television. *American Economic Review: Insights*, 5(2):207–223.

Kraay, A. and McKenzie, D. (2014). Do poverty traps exist? assessing the evidence. *Journal of Economic Perspectives*, 28(3):127–148.

Liadze, I., Macchiarelli, C., Mortimer-Lee, P., and Sanchez Juanino, P. (2023). Economic costs of the Russia-Ukraine war. *The World Economy*, 46(4):874–886.

Lin, E. (2022). How war changes land: soil fertility, unexploded bombs, and the underdevelopment of Cambodia. *American Journal of Political Science*, 66(1):222–237.

Miguel, E. and Roland, G. (2011). The long-run impact of bombing Vietnam. *Journal of Development Economics*, 96(1):1–15.

Nagengast, A. J. and Yotov, Y. V. (2025). Staggered difference-in-differences in gravity settings: Revisiting the effects of trade agreements. *American Economic Journal: Applied Economics*, 17(1):271–296.

Riaño, J. F. and Valencia Caicedo, F. (2024). Collateral damage: the legacy of the secret war in Laos. *The Economic Journal*, 134(661):2101–2140.

Roberts, M. (2021). Tracking economic activity in response to the COVID-19 crisis using nighttime lights–the case of Morocco. *Development Engineering*, 6:100067.

Rose, A., Chen, Z., and Wei, D. (2023). The economic impacts of Russia-Ukraine war export disruptions of grain commodities. *Applied Economic Perspectives and Policy*, 45(2):645–665.

Roshan, G., Ghanghermeh, A., Sarli, R., and Grab, S. W. (2024). Environmental impacts of shifts in surface urban heat island, emissions, and nighttime light during the Russia–Ukraine war in Ukrainian cities. *Environmental Science and Pollution Research*, 31(32):45246–45263.

Roth, J., Sant'Anna, P. H., Bilinski, A., and Poe, J. (2023). What's trending in difference-in-differences? a synthesis of the recent econometrics literature. *Journal of Econometrics*, 235(2):2218–2244.

Sachs, J. D. (2006). *The end of poverty: economic possibilities for our time*. Penguin.

Saing, C. H. and Kazianga, H. (2020). The long-term impacts of violent conflicts on human capital: US bombing and, education, earnings, health, fertility and marriage in Cambodia. *The Journal of Development Studies*, 56(5):874–889.

Schmidheiny, K. and Siegloch, S. (2019). On event study designs and distributed-lag models: Equivalence, generalization and practical implications. Technical Report n. 7481, CESifo Working Paper.

Shen, Z., Zhu, X., Cao, X., and Chen, J. (2019). Measurement of blooming effect of DMSP-OLS nighttime light data based on NPP-VIIRS data. *Annals of GIS*, 25(2):153–165.

Sun, L. and Abraham, S. (2021). Estimating dynamic treatment effects in event studies with heterogeneous treatment effects. *Journal of Econometrics*, 225(2):175–199.

Tveit, T., Skoufias, E., and Strobl, E. (2022). Using VIIRS nightlights to estimate the impact of the 2015 Nepal earthquakes. *Geoenvironmental Disasters*, 9(1):1–13.

Uprety, S., Cao, C., Gu, Y., Shao, X., Blonski, S., and Zhang, B. (2019). Calibration improvements in S-NPP VIIRS DNB sensor data record using version 2 reprocessing. *IEEE Transactions on Geoscience and Remote Sensing*, 57(12):9602–9611.

Yamada, T. and Yamada, H. (2021). The long-term causal effect of us bombing missions on economic development: evidence from the Ho Chi Minh Trail and Xieng Khouang Province in Lao PDR. *Journal of Development Economics*, 150:102611.

Supplementary tables and figures (Appendix)

Estimating the economic impact of the Russia-Ukraine conflict with nightlights data

L. Buzzacchi[a,*], A.M. De Marco[a], F.L. Milone[a]

[a] *Politecnico di Torino, Interuniversity Department of Regional and Urban Studies and Planning*

[*] Corresponding author:
Prof. Luigi Buzzacchi (luigi.buzzacchi@polito.it), Interuniversity Department of Regional and Urban Studies and Planning, Politecnico di Torino; Viale Mattioli 39, 10125, Torino, Italy.

1. Appendix A1. Allocation of Municipalities to Raions.

The original Raions' division counts 620 unique areas, divided in 498 Raions and 112 Municipalities (*Misto* or *Mis'ka Rada*). In the original file, in fact, 112 municipalities pertaining to a given Raion are classified as separate entities (from the Raion itself) at the same administrative level of canonical Raions.[1]

To build a unique dataset, and to control for the presence of potential spatial spillovers, we decided to reorganize the entities in our data, using the following rule:

1. if the municipality is in the center of a Raion and its area is totally included in the corresponding Raion, we annexed the municipality onto the Raion;

2. otherwise, if the municipality is sharing only a border with the corresponding Raion, we treated the municipality as separate entity.

In the following Figure 1 we show two auxiliary examples, showing the allocation processes of municipalities to corresponding Raions: in Panel (a) the original municipality is annexed to the corresponding Raion (pertaining to point 1. above), in Panel (b) it is treated as a separate entity (hence, referring to point 2. above).

As a result, we built a final database based on 515 Raions, later restricted to 473 to exclude those under Russian control.

[1] In the sense, it is worth to note that not all Raions have the main city recorded as a separate entity.

Figure 1: Allocation of Municipalities to Raions.

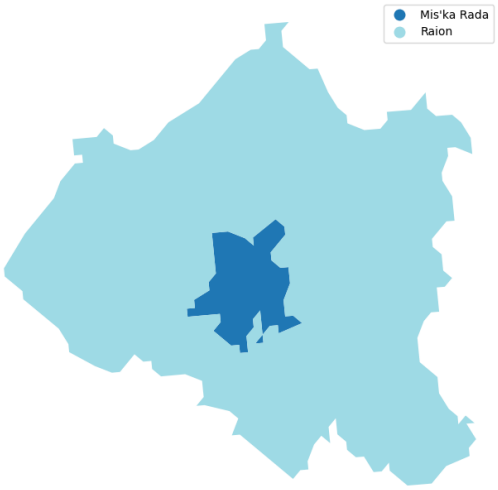

(a) Case 1: the municipality is annexed to the Raion.

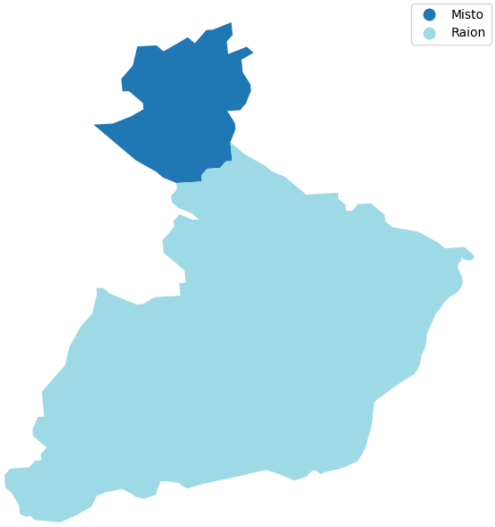

(b) Case 2: the "municipality" is treated as a separate entity.

2. Appendix A2. Cross-sectional univariate correlation between night-light intensity and GRP (at the Oblast level).

In Figure 2 we show the univariate correlation between observed night-light density (*asinh* transformed) and Gross Regional Product. Data are at the Oblast level and are defined as follows: *DensLight* = mean value of night-light density in 2019, *GRP* = Oblasts' level Gross Regional Product at 2013. We opted for such a year given that our geographical division refers to the oldest classification.

The estimated univariate elasticity is 0.74, with a standard error of 0.16 (p-value < 0.000) and an R2 of 0.50. The point on the top right is the Oblast of Kiev City, which is, as expected, characterized by the largest economic activity, and hence, by the largest night-light values. For the sake of clarity, the univariate correlation remains robust even if we omit this oblast (Kiev City) from the analysis (elasticity = 1.22, std. err = 0.37, p $<$ 0.003).

Figure 2: *Asinh* of night-light intensity vs *asinh* of Gross Regional Product (at the Oblast level).

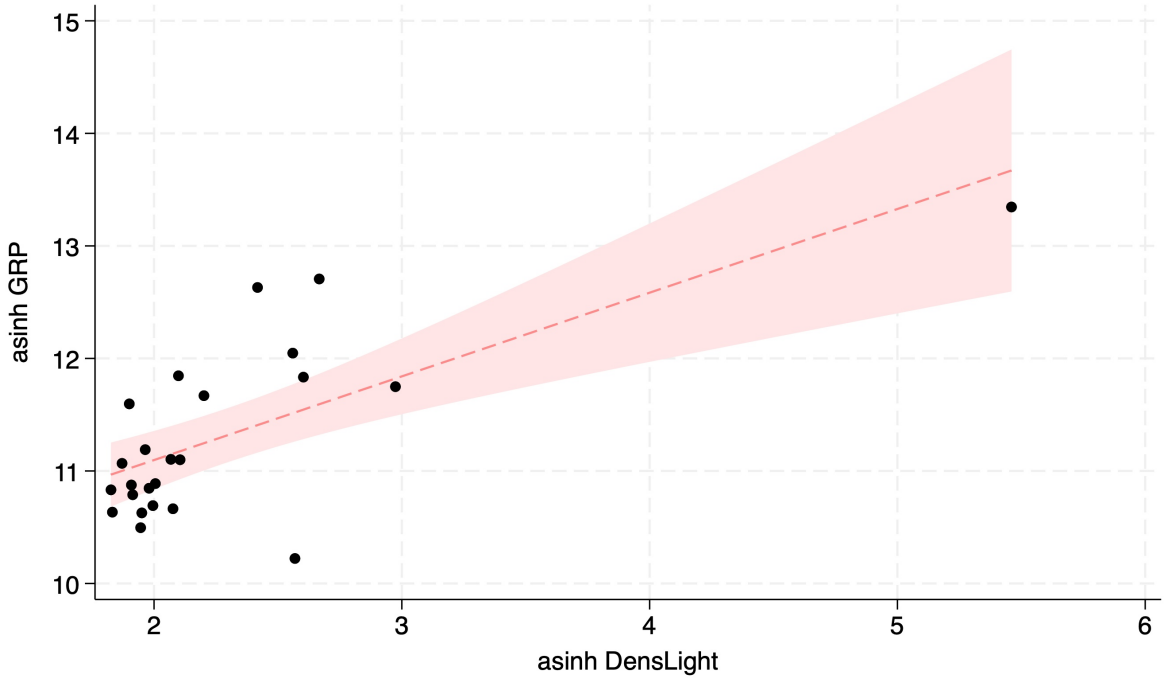

Notes: a) The red-dashed line is the univariate OLS-fitted regression line; b) red area shows the 95% confidence interval; c) each point is an Oblast.

3. Appendix A3. Evolution of $MedLight_{it}$ over time.

Figure 3: Temporal evolution of *MedLight*.

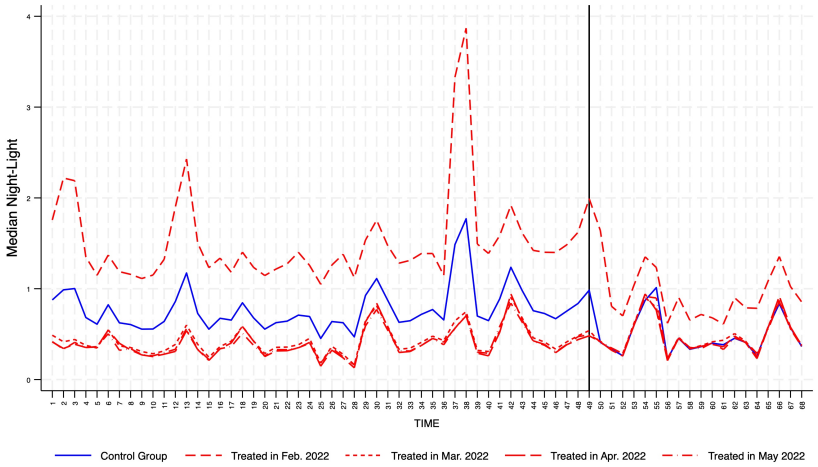

(a) y = $MedLight_{it}$

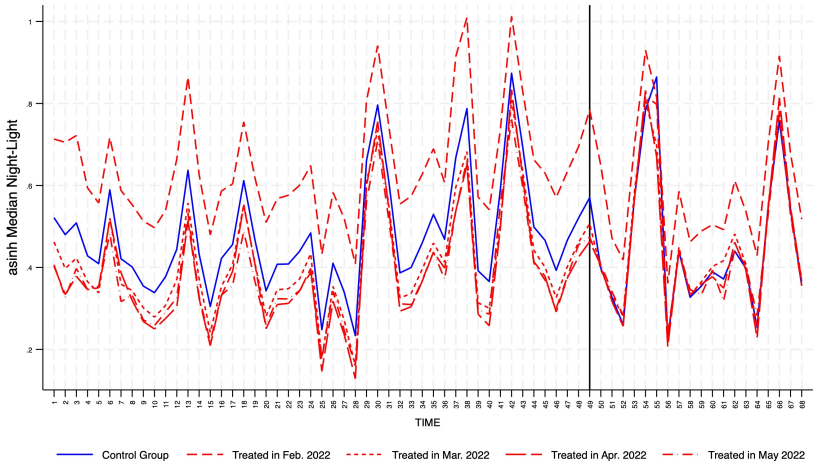

(b) y = $asinh\ MedLight_{it}$

In Figure 3 we show the within group mean values of $MedLight_{it}$ (defined as the night-light intensity of the median pixel in Raion i at year-month t). *Control group* contains Raions not yet treated at the corresponding point in time (hence both never treated and not yet ones). The four largest treatment cohorts are shown; d) vertical reference line T = 49 = January 2022 (one period before conflict begins).

4. Appendix A4. Baseline TWFE estimates using $MedLight_{it}$ as dependent variable.

Table 1: Baseline TWFE estimates using $MedLight_{it}$ as dependent variable.

	y = $MedLight_{it}$			**y** = ***asinh*** $MedLight_{it}$		
	M1.1	**M1.2**	**M1.3**	**M2.1**	**M2.2**	**M2.3**
$Conflict_{it}$	-0.086**	-0.141**	-0.030*	-0.041***	-0.040***	-0.022***
	(0.037)	(0.070)	(0.017)	(0.009)	(0.010)	(0.006)
$asinh\ Temperature_{it}$	-414.921+		-456.542+	-100.299**		-117.346**
	(264.544)		(292.395)	(42.601)		(46.273)
$asinh\ Temperature_{it}$	32.383+		35.669	7.740**		9.088**
	(20.733)		(22.930)	(3.347)		(3.636)
$asinh\ Rainfalls_{it}$	0.002		0.004	-0.001		-0.001
	(0.002)		(0.004)	(0.001)		(0.001)
$asinh\ WindSpeed_{it}$	-0.037***		-0.020	-0.030***		-0.025***
	(0.011)		(0.017)	(0.007)		(0.007)
FRP_{it}		0.004***	0.001		-0.000**	-0.000
		(0.002)	(0.001)		(0.000)	(0.000)
$asinh\ AntiAirDefence_{it}$		-0.406*	-0.132		-0.055**	-0.044*
		(0.209)	(0.102)		(0.022)	(0.023)
Constant	1329.448+	0.785***	1461.201+	325.293**	0.498***	379.179**
	(843.836)	(0.013)	(932.037)	(135.558)	(0.002)	(147.230)
Raion FE	Yes	Yes	Yes	Yes	Yes	Yes
Time FE	Yes	Yes	Yes	Yes	Yes	Yes
N	31,144	32,164	31,144	31,144	32,164	31,144
R2	0.646	0.782	0.652	0.811	0.922	0.816
Within R2	0.005	0.017	0.022	0.013	0.037	0.035

Notes: a) *** p<0.01, ** p<0.05, * p<0.10, b) clustered standard errors at the Raion level in parentheses.

In Table 1 we show the baseline TWFE OLS estimates (according to Equation 1 in the main manuscript) using $MedLight_{it}$ as dependent variable.

As per the main results, using $DensLight_{it}$, in all regressions, the average treatment effect associated to the variable $Conflict_{it}$ is always negative and statistically significant. We estimate that in treated Raions, following the first military event, the average decline of night-light intensity at the median pixel ranges from -0.030 to –0.141 in levels. In relative terms (see models M2.1 to M2.3) the estimated elasticity of is in the range between -2.2% and -4.0%[2].

We return in Section 5.2. of the main manuscript of the reasons why such an elasticity is lower compared to the elasticity computed when $DensLight_{it}$ is used as dependent variable.

[2] Estimated as $e^{\beta} - 1$.

5. Appendix A5. Additional specification with additional seasonality effects.

Table 2: Baseline TWFE estimates using $MedLight_{it}$ as dependent variable.

	Y = $DensLight_{it}$	Y = *asinh* $DensLight_{it}$	Y = $MedLight_{it}$	Y = *asinh* $MedLight_{it}$	Y = $DensLight_{it}$	Y = *asinh* $DensLight_{it}$	Y = $MedLight_{it}$	Y = *asinh* $MedLight_{it}$
	M1	**M2**	**M3**	**M4**	**M5**	**M6**	**M7**	**M8**
$Conflict_{it}$	-0.679***	-0.084***	-0.026	-0.020***	-0.685***	-0.082***	-0.027+	-0.019***
	(0.240)	(0.018)	(0.017)	(0.006)	(0.238)	(0.018)	(0.017)	(0.006)
asinh $Temperature_{it}$	-1.05e+04***	-1290.007***	-883.249***	-431.200***	-1.38e+04***	-1809.599***	-1120.915***	-613.170***
	(2732.865)	(133.611)	(283.233)	(49.922)	(2736.544)	(93.183)	(259.665)	(41.284)
asinh $Temperature_{it}^2$	823.904***	101.441***	69.604***	33.978***	1086.953***	142.462***	88.364***	48.351***
	(215.227)	(10.545)	(22.316)	(3.935)	(215.370)	(7.342)	(20.441)	(3.251)
asinh $Rainfalls_{it}$	-0.006	-0.014***	0.002	-0.002+	0.003	-0.011***	0.002	-0.001
	(0.029)	(0.003)	(0.003)	(0.001)	(0.025)	(0.003)	(0.002)	(0.001)
asinh $WindSpeed_{it}$	-0.198	-0.095***	-0.004	-0.015**	-0.244	-0.101***	0.001	-0.016**
	(0.175)	(0.019)	(0.015)	(0.006)	(0.188)	(0.018)	(0.019)	(0.006)
FRP_{it}	0.012*	-0.000	0.001	0.000	0.007	-0.000	0.000	-0.000
	(0.007)	(0.000)	(0.001)	(0.000)	(0.005)	(0.000)	(0.001)	(0.000)
asinh $AntiAirDefenceit$	-1.860**	-0.132***	-0.131	-0.044*	-1.832**	-0.132***	-0.130	-0.043*
	(0.853)	(0.030)	(0.102)	(0.023)	(0.846)	(0.030)	(0.101)	(0.023)
Constant	33273.808***	4103.309***	2802.456***	1368.466***	43831.978***	5748.624***	3555.146***	1944.431***
	(8674.934)	(423.213)	(898.664)	(158.333)	(8692.507)	(295.640)	(824.608)	(131.081)
Seasonality	Oblast × Season FE				Raion × Season FE			
Raion FE	Yes	Yes	Yes	Yes	Yes	Yes	Yes	Yes
Time FE	Yes	Yes	Yes	Yes	Yes	Yes	Yes	Yes
N	31,144	31,144	31,144	31,144	31,144	31,144	31,144	31,144
R2	0.741	0.846	0.669	0.829	0.775	0.861	0.715	0.840
Within R2	0.045	0.072	0.022	0.036	0.050	0.081	0.025	0.040

Notes: a) *** p<0.01, ** p<0.05, * p<0.10, b) clustered standard errors at the Raion level in parentheses.

In Table 2 we show the baseline TWFE OLS estimates (according to Equation 1 in the main manuscript) using $DensLight_{it}$ and $MedLight_{it}$ (in both linear and *asinh* transformation) as dependent variables, with additional seasonal fixed effects. Models M1 to M4 absorb Oblast times Season (defined as calendar seasons, i.e., Winter, Spring, Summer, Autumn) fixed effects, hence controlling for season-specific shocks at the regional level. In this sense, the interpretation of the average treatment effect can be intended cœteris paribus both time fixed effects (capturing common shocks to the whole Ukraine) and regional specific seasonality-driven shocks capturing either economic-related factors or weather related ones (not accounted in our control variables) that could affect the observed night-light in a given period. Models M5 to M8 are even more restrictive, since they absorb Raion times Season fixed effects.

We show that the average treatment effect associated to the variable $Conflict_{it}$ remains negative and statistically significant, with a magnitude similar to the estimates without additional seasonal fixed effects. In the most restrictive specifications using log-log transformed variables, we find $DensLight_{it}$ to be about 8% lower in treated Raions following the first military event (i.e., $Conflict_{it} = 1$) (M6),[3] while $MedLight_{it}$ is about 2% lower (M8).[4] Given that the coefficients are rather stable, in all the following estimates we will stick to the baseline models without additional seasonality fixed effects, which are most likely already accounted by time fixed effects and weather-related controls.

[3] Computed as $e^{-0.082} - 1 = -0.08$.
[4] Computed as $e^{-0.019} - 1 = -0.018$.

6. Appendix A6. Decomposition of the average treatment effect according to Goodman-Bacon (2021).

Table 3: Goodman-Bacon (2021) decomposition of the average treatment effect using $DensLight_{it}$ as dependent variable.

	y = $DensLight_{it}$		y = $asinh\ DensLight_{it}$	
	Beta	**Weight**	**Beta**	**Weight**
Timing Groups	-0.463	18%	-0.070	18%
Never vs Timing Groups	-1.576	76%	-0.151	76%
Within	9.730	6%	0.661	6%
Average Treatment Effect	-0.706***		-0.088***	
	(0.097)		(0.006)	

Notes: a) *** p<0.01, ** p<0.05, * p<0.10; b) all control variables and TWFE are included, resembling to the same specification of Models M1.3 and M2.3 in Table 5 of the manuscript.

Table 4: Goodman-Bacon (2021) decomposition of the average treatment effect using $MedLight_{it}$ as dependent variable.

	y = $DensLight_{it}$		y = $asinh\ DensLight_{it}$	
	Beta	**Weight**	**Beta**	**Weight**
Timing Groups	-0.041	18%	-0.025	18%
Never vs Timing Groups	-0.088	76%	-0.041	76%
Within	0.748	6%	0.239	6%
Average Treatment Effect	-0.030***		-0.022***	
	(0.010)		(0.003)	

Notes: a) *** p<0.01, ** p<0.05, * p<0.10; b) all control variables and TWFE are included, resembling to the same specification of Models M1.3 and M2.3 in Table 1 (Appendix A4).

In Tables 3 and 4 we provide the decomposition of the average treatment effect according to Goodman-Bacon (2021). The interpretation is as follows. First, the Tables show the overall Average Treatment Effect: it is worth to note that, since these models include all control variables and TWFE, these estimates are, indeed, equivalent to those reported in Models M1.3 and M2.3 of Table 5 in the main manuscript and Table 1 in Appendix 4. Second, the Tables show the decomposition of such Average Treatment Effect according to three distinct possibilities:

- Timing Groups: Raions whose treatment – i.e., first military event – was allocated at different times, such that they can serve as each other's controls groups in two ways. On the one hand, those treated later can serve as the control group for an earlier treatment group. On the other hand, those treated earlier serve as the control group for the later group. While under the assumption of no anticipatory effects and parallel trends the first alternative is a valid comparison, the second alternative is what Goodman-Bacon (2021) states as *forbidden comparisons* given that in such a case we would be comparing Raions already attacked (as control group) with those experiencing an attack for the first time.

- Never vs Timing Groups: Never treated indicates a group which never receives the treatment serves as the control group for all the timing groups. This is, by definition, a good comparisons.
- Within is the residual component.

Each comparison has its own estimated Average Treatment Effect and the corresponding weight, such that the overall Average Effect is a weighted average of the three of them.

We show that most of the estimated Average Treatment Effect comes from *good comparisons*, since in all cases around 76% of the estimate is coming from the comparison with never treated Raions.

This evidence suggest that biases of the canonical OLS TWFE could be limited in our setting. Indeed, this is in line with the descriptive evidence on the allocation of the attacks, which shows that almost all treated Raions have been treated in the first four months of the conflict. Nonetheless, there is still a residual unobserved comparisons between earlier and late treated Raions (the *forbidden comparisons*) which may underestimate our overall Average Treatment Effect given that comparing late attacked Raions with those already attacked (and which already experienced a decline in night-light intensity) may produce positive estimates. For this reason, Section 4.3. of the manuscript we provide estimates using Borusyak et al. (2024) and Callaway and Sant'Anna (2021) that are robust to such an issue, and in Section 5.1. we resort to De Chaisemartin and d'Haultfoeuille (2024) which provides a robust estimator in the staggered design with repeated and not absorbing treatment.

7. Appendix A7. Estimates with Borusyak et al. (2024) and Callaway and Sant'Anna (2021) using $MedLight_{it}$ as dependent variable.

Table 5: Estimates with estimators for staggered design ($MedLight_{it}$ as dependent variable).

	Borusyak et al. - BJS					
	y = $MedLight_{it}$			y = $asinh\ MedLight_{it}$		
	M1.1	**M1.2**	**M1.3**	**M2.1**	**M2.2**	**M2.3**
$Conflict_{it}$	-0.091**	-0.348***	-0.088**	-0.043***	-0.064***	-0.039***
	(0.039)	(0.109)	(0.040)	(0.010)	(0.013)	(0.011)
Controls *weather-related*	Yes	No	Yes	Yes	No	Yes
Controls *conflict-related*	No	Yes	Yes	No	Yes	Yes
Raion FE	Yes	Yes	Yes	Yes	Yes	Yes
Time FE	Yes	Yes	Yes	Yes	Yes	Yes
N	31,144	32,164	31,144	31,144	32,164	31,144
	Callaway & Sant'Anna - CS					
	y = $MedLight_{it}$			y = $asinh\ MedLight_{it}$		
	M3.1	**M3.2**	**M3.3**	**M4.1**	**M4.2**	**M4.3**
$Conflict_{it}$	-0.156**	-0.549***	-0.155**	-0.064***	-0.101***	-0.064***
	(0.061)	(0.161)	(0.061)	(0.015)	(0.018)	(0.015)
Controls *weather-related*	Yes	No	Yes	Yes	No	Yes
Controls *conflict-related*	No	Yes	Yes	No	Yes	Yes
Raion FE	Yes	Yes	Yes	Yes	Yes	Yes
Time FE	Yes	Yes	Yes	Yes	Yes	Yes
N	31,144	32,164	31,144	31,144	32,164	31,144

Notes: a) *** p<0.01, ** p<0.05, * p<0.10, b) clustered standard errors at the Raion level in parentheses, c) BJS stands for Borusyak et al. (2024) estimator, d) CS stands for Callaway and Sant'Anna (2021) estimator and employed not-yet treated Raions as control group; e) Controls *weather-related* contains: $Temperature_{it}$ (in linear and quadratic terms), $Rainfalls_{it}$ and $WindSpeed_{it}$; f) Controls *conflict-related* contains: FRP_{it} and $AntiAirDefence_{it}$.

As per the estimates using $DensLight_{it}$ as dependent variable, even when using $MedLight_{it}$ we find that staggered difference-in-differences estimators produce way larger estimates in magnitude.

However, in this case, the estimates provided by Callaway and Sant'Anna (2021) are double than those provided by Borusyak et al. (2024). In fact, when using Callaway and Sant'Anna (2021) we find that following the first military event, there is a decrease in night-light luminosity (proxied by median) of about 6%.[5] Conversely, when using Borusyak et al. (2024), the estimates lowers to about 4%.[6].

In any case, these estimates are less than half compared to those reported in the main manuscript using $DensLight_{it}$ as dependent variable. Again, in Section 5.2. of the manuscript we return on the rationale behind such a difference.

[5] Computed as $e^{-0.064} - 1 = -0.062$.
[6] Computed as $e^{-0.039} - 1 = -0.038$.

8. Appendix A8. Event study estimates using $DensLight_{it}$ as dependent variable.

Figure 4: Event study plot. y = $DensLight_{it}$.

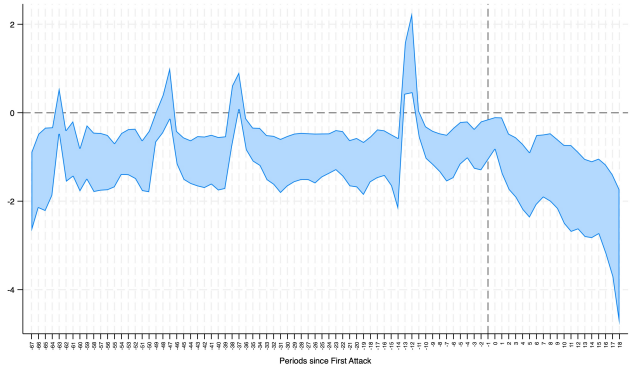

(a) Canonical TWFE OLS estimator.

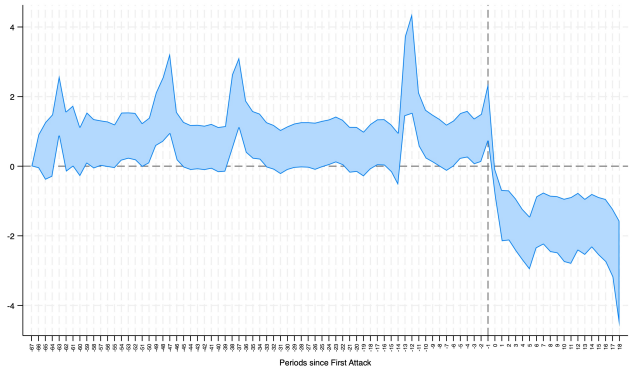

(b) Borusyak et al. estimator.

(c) Callaway & Sant'Anna estimator.

Notes: a) 95% confidence interval based on clustered robust standard errors at the Raion level is shown; b) the vertical line (dash line) refers to one month before the treatment (i.e., first military event).

9. Appendix A9. Event study estimates using $MedLight_{it}$ as dependent variable.

Figure 5: Event study plot. y = $MedLight_{it}$.

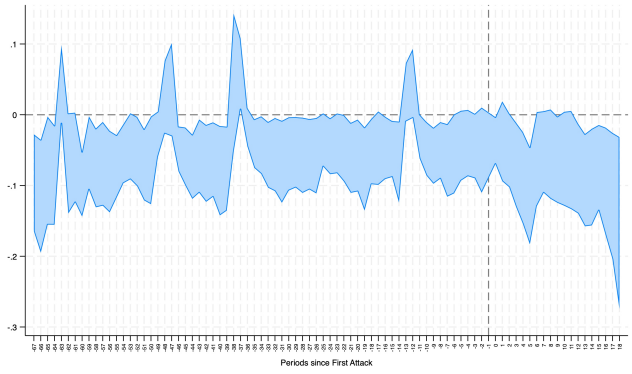

(a) Canonical TWFE OLS estimator.

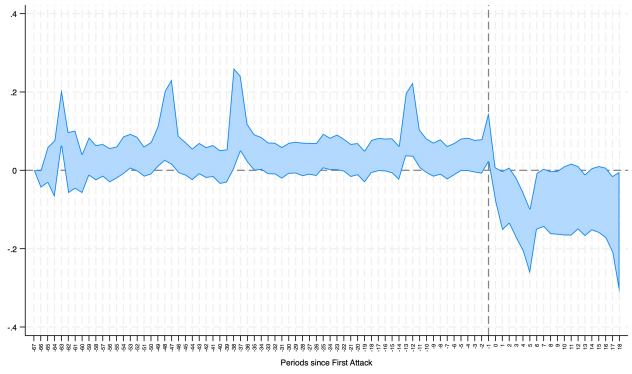

(b) Borusyak et al. estimator.

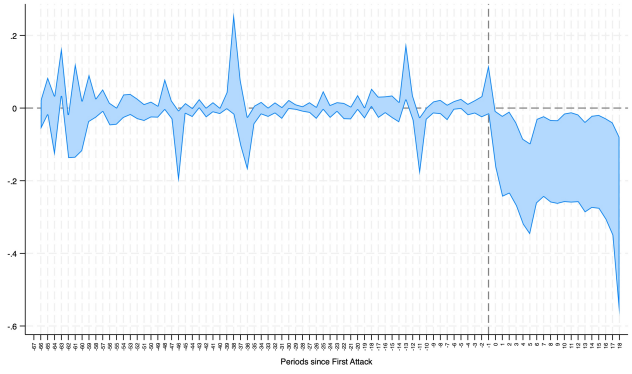

(c) Callaway & Sant'Anna estimator.

Notes: a) 95% confidence interval based on clustered robust standard errors at the Raion level is shown; b) the vertical line (dash line) refers to one month before the treatment (i.e., first military event).

10. Appendix A10. Event study estimates using $asinh\ MedLight_{it}$ as dependent variable.

Figure 6: Event study plot. y = $asinh\ MedLight_{it}$.

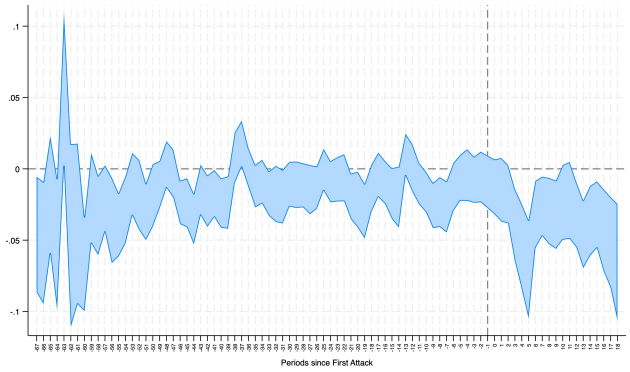

(a) Canonical TWFE OLS estimator.

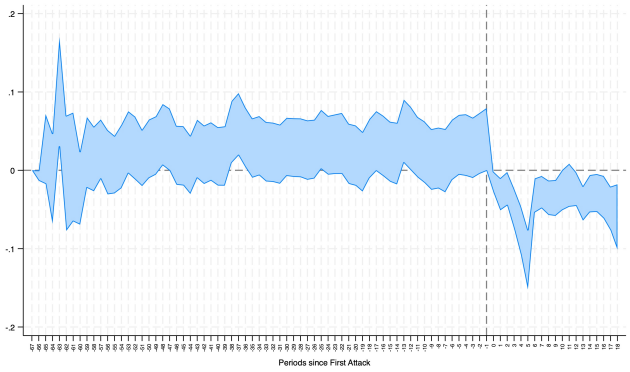

(b) Borusyak et al. estimator.

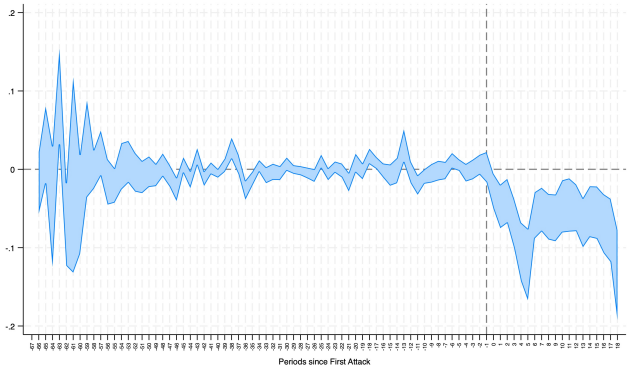

(c) Callaway & Sant'Anna estimator.

Notes: a) 95% confidence interval based on clustered robust standard errors at the Raion level is shown; b) the vertical line (dash line) refers to one month before the treatment (i.e., first military event).

11. Appendix A11. Temporal evolution of $Events_{it}$.

Figure 7: Number of military events ($Events_{it}$) over time.

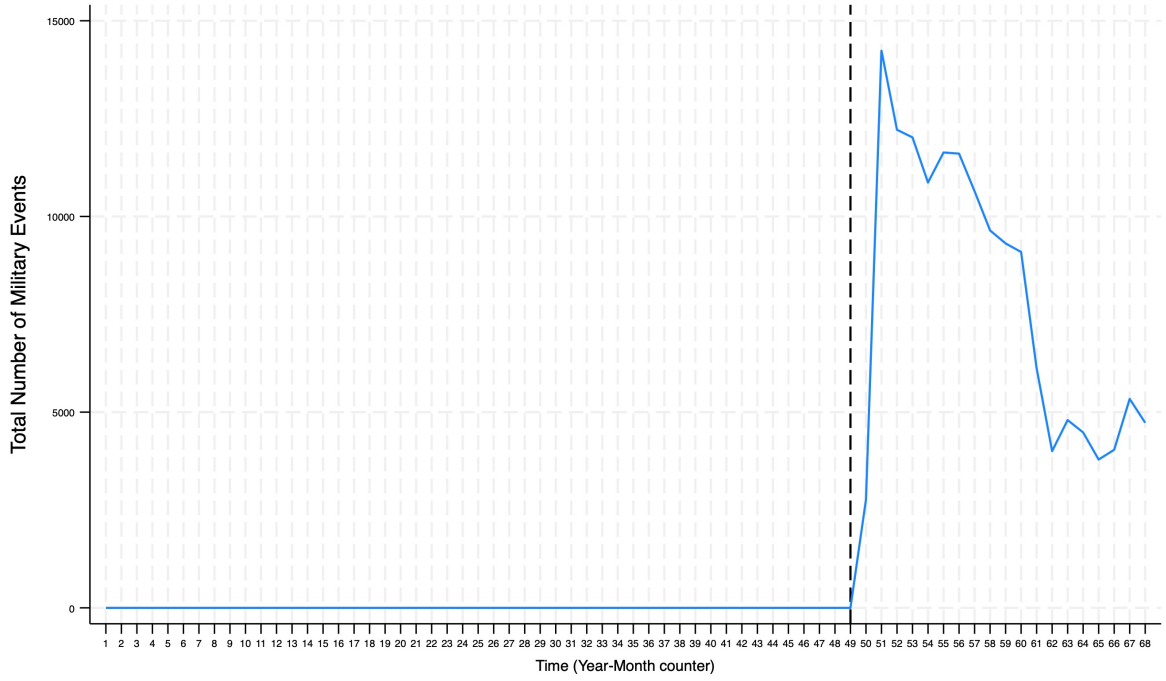

Notes: a) Number of military events (net of anti-air defense events in shown); b) the vertical reference line indicate the month of January 2022 (one month before the conflict begins.

Figure 7 shows the temporal distribution of the number of military events (i.e., the variable $Events_{it}$). Most of the events have been allocated in the first months of the conflict, indeed up to September 2022 more than 10,000 military events per month have been recorded. The numbers harshly feel in February 2023, indeed, the mean monthly number of events in the last months of our panel is about 5,000 (about on third of the peak reached in March 2022).

12. Appendix A12. Baseline Continuous Treatment Design using $MedLight_{it}$ as dependent variable.

Table 6: Baseline continuous treatment design using $MedLight_{it}$ as dependent variable.

	y = $MedLight_{it}$			y = ***asinh*** $MedLight_{it}$		
	M1.1	**M1.2**	**M1.3**	**M2.1**	**M2.2**	**M2.3**
$Conflict_{it}$	0.012	-0.075	-0.004	-0.004	-0.023**	-0.009
	(0.038)	(0.055)	(0.024)	(0.010)	(0.010)	(0.007)
$Conflict_{it}$× $asinh\ Events_{it}$	-0.059	-0.063*	-0.025**	-0.022**	-0.017***	-0.013***
	(0.041)	(0.034)	(0.012)	(0.009)	(0.005)	(0.004)
Constant	1455.882+	0.783***	1470.846+	371.917**	0.498***	384.072***
	(925.706)	(0.013)	(935.443)	(145.778)	(0.002)	(147.612)
Controls *weather-related*	Yes	No	Yes	Yes	No	Yes
Controls *conflict-related*	No	Yes	Yes	No	Yes	Yes
Raion FE	Yes	Yes	Yes	Yes	Yes	Yes
Time FE	Yes	Yes	Yes	Yes	Yes	Yes
N	31,144	32,164	31,144	31,144	32,164	31,144
R2	0.651	0.782	0.652	0.816	0.922	0.816
Within R2	0.019	0.018	0.023	0.035	0.041	0.038

Notes: a) *** p<0.01, ** p<0.05, * p<0.10, + p<0.12; b) clustered standard errors at the Raion level in parentheses; c) Controls *weather-related* contains: $Temperature_{it}$ (in linear and quadratic terms), $Rainfalls_{it}$ and $WindSpeed_{it}$; d) Controls *conflict-related* contains: FRP_{it} and $AntiAirDefence_{it}$.

Table 6 reports that if we use the median of night-light as dependent variable, the average treatment effect common to all treated Raions ($Conflict_{it}$) is negative, yet not always significant. Conversely, the treatment effect imputed to treatment intensity heterogeneity is significant, and suggests that doubling the number of events in a Raions decreases observed median light intensity by around 1%.[7]

As per the static estimates, the median is rather less elastic to the conflict compared to the average density of night-light. In Section 5.2. of the manuscript we provide an intuition on this.

[7] Computed as $2^{-0.013} - 1 = 0.008$ using the estimates in M2.3.

13. Appendix A13. Heterogeneous treatment *dosages*.

Table 7: Number of military events at treatment allocation date (T = 0).

$Events_{iT=0}$	# of Raions	% of Raions	Cum. % of Raions
1 to 5	241	71.30%	71.30%
6 to 25	66	19.53%	90.83%
26 to 100	27	7.99%	98.82%
101 to 1216	4	1.18%	100.00%
Total	338	100.00%	

Notes: a) the number of the events at the first month a treated Raion is attacked is shown.

Table 8: Change in treatment dosage ($Events_{it} - Events_{it-1}$) from T=1 onward.

$Events_{it} - Events_{it-1}$	# Raion-month obs.	% Raion-month obs.	Cum. % Raion-month obs.
-101 to -733	74	1.35%	1.35%
-26 to -100	210	3.83%	5.19%
-6 to -25	494	9.02%	14.21%
-1 to -5	970	17.71%	31.92%
0	2,253	41.14%	73.06%
1 to 5	776	14.17%	87.24%
6 to 25	416	7.60%	94.83%
26 to 100	209	3.82%	98.65%
101 to 1216	74	1.35%	100.00%
Total	5,476	100.00%	

Notes: a) the difference in the number of the events from one period to the previous one (excluding T=0) is shown.

14. Appendix A14. Treatment paths.

Table 9: Baseline TWFE estimates using $MedLight_{it}$ as dependent variable.

Max. consecutive months with $Events_{it} > 0$	**# Raions**	**% Raions**	**Events per Raion-Month**	**# Raions with Persistent Treatment**	**Avg. Treat. Interrupt.**	**Min. Treat. Interrupt.**	**Max. Treat. Interrupt.**
0	97	28.70%	0.158	2	1.46	0	5
1	44	13.02%	0.535	1	2.27	0	5
2	20	5.92%	1.667	0	3.60	1	6
3	15	4.44%	1.663	0	3.33	2	6
4	10	2.96%	2.833	0	3.90	2	5
5	12	3.55%	4.236	0	3.00	1	5
6	11	3.25%	4.737	0	3.00	1	6
7	8	2.37%	6.028	0	3.00	2	4
8	5	1.48%	7.133	0	3.00	2	4
9	5	1.48%	4.989	0	2.00	1	3
10	9	2.66%	11.383	0	1.44	1	3
11	4	1.18%	15.375	0	1.75	1	2
12	5	1.48%	11.156	0	1.80	1	2
13	8	2.37%	9.819	0	1.38	1	2
14	4	1.18%	17.931	0	1.50	1	2
15	4	1.18%	13.736	0	1.00	1	1
16	4	1.18%	14.153	1	0.75	0	1
17	9	2.66%	36.346	7	0.22	0	1
18	64	18.93%	113.467	64	0.00	0	0
Total	338	100.00%	24.875	75	1.70	0	6

Notes: a) Persistent Treatment = Raions in which when the treatment turns off, it never becomes positive again; b) Treat. Interrupt. stands for treatment interruptions = mean treatment interruptions (i.e., from positive to zero).

In Table 9 we show the distribution of treated Raions according to the longest period of consecutive treatments (i.e., consecutive months where the variable $Events_{it}$ takes a value greater than 0).

In 97 Raions we never find two consecutive months with a positive treatment. Among these 97 Raions, only two of them recorded a persistent treatment (i.e., after the treatment turns off, it will never become again positive).

On the opposite side, 64 Raions have been continuously treated from February 22 up to August 2023 (indeed in such a case we find that all these Raions are classified as persistent treatment and there is never a treatment interruption).

In the average Raion the treatment has been interrupted 1.70 times, however we also find cases in which military events in a Raions have been interrupted from one month to the other up to 6 times. Naturally, such a number is lower (and takes values around 1 or 0) in Raions continuously treated for longer periods of time (> 15). According to the length of the exposure to the treatment, it is also rather evident that the longest is the period under cumulative attacks, the largest is the mean number of events in the corresponding Raion.

15. Appendix A15. Canonical Event Study Estimates using De Chaisemartin and d'Haultfoeuille (2024) as estimator and *asinh* $DensLight_{it}$ as dependent variable.

Figure 8: Canonical Event Study Estimates using De Chaisemartin and d'Haultfoeuille (2024) as estimator and *asinh* $DensLight_{it}$ as dependent variable.

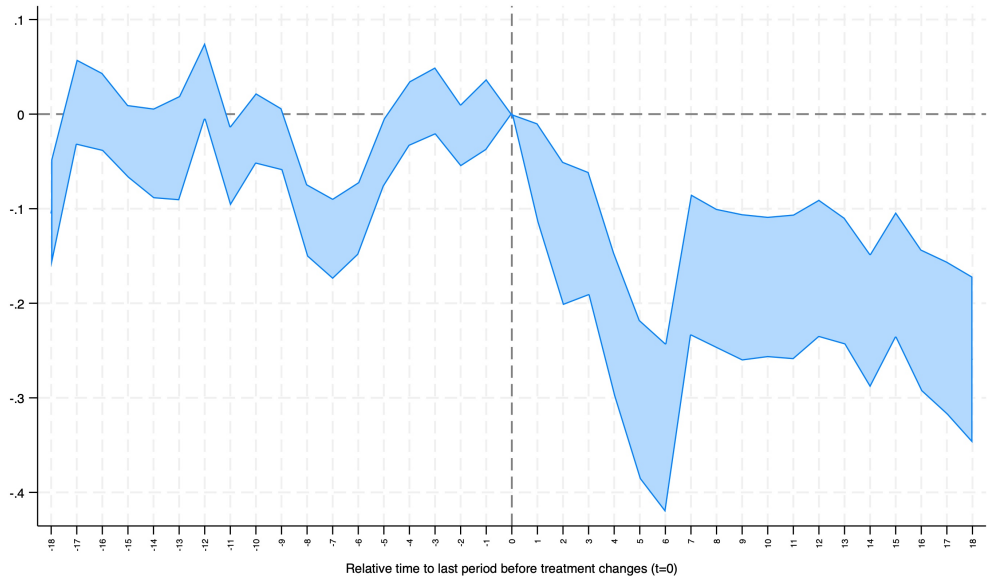

Notes: a) 95% confidence interval based on clustered robust standard errors at the Raion level is shown; b) the vertical line (dash line) refers to one month before the treatment (i.e., first military event).

Figure 8 reports the canonical event study estimates using the estimator proposed by De Chaisemartin and d'Haultfoeuille (2024). Compared to the estimates presented in Figure 3 of the main manuscript and Appendixes 8, 9 and 10, T = 0 in this graph corresponds to one period before *first* treatment change.[8] In other words, the count of the relative time axis is shifted by one position on the left, still the interpretation is similar as each lag can be interpreted as the average treatment effect on the treated at a given period from the first military event. Furthermore, by construction, De Chaisemartin and d'Haultfoeuille (2024) allows to estimate a number of placebo coefficients up to the number of lags, hence with such an estimator we could only fit 18 pre-treatment leads.

Concerning the post-treatment estimates, we find that results are in *pattern* similar to OLS TWFE, Borusyak et al. (2024) and Callaway and Sant'Anna (2021). In magnitude, the estimates are instead close and adherent to those proposed by Borusyak et al. (2024) and Callaway and Sant'Anna (2021). This is not surprising, since De Chaisemartin and d'Haultfoeuille (2024) is designed to deal with *staggered* designs, hence it is suitable to

[8] In the other estimates, instead, it corresponds to T = -1.

control for the presence of forbidden comparisons in the estimation of the average treatment effect.

Concerning pre-treatment leads, the estimator suggested not significant differences between treated and control Raions in the immediate surroundings before the first military event (up 6 months before the first attack), and in longer leads (-18 to -9). In the middle we find a significant (negative) difference, not remarkably evidenced by Borusyak et al. (2024) and Callaway and Sant'Anna (2021). However, no clear patterns before the treatment allocation can be detected in the graph (Freyaldenhoven et al., 2021).

16. Appendix A16. Normalized weights employed by De Chaisemartin and d'Haultfoeuille (2024) to estimate the average marginal effect of $Events_{it}$ by temporal lag (Figure 4 of the manuscript).

In Table 10 we show the weights used by De Chaisemartin and d'Haultfoeuille (2024) to estimate the *normalized* event study plot in Figure 4 of the manuscript. As can be seen, the event-study estimate at $l = +1$ (first period in which treatment changes, i.e., there are new military events) is the average marginal effect of these contemporaneous military events on night-light intensity (indeed there is only one possible event lead $k=0$ with a wieght of 100%). The second *normalized* effect (at $l = +2$) is the weighted average of the effects of contemporaneous events and of the first lag of of events on night-light intensity (those allocated in the previous period). As we move further on l, we show that weights are approximately equal for all leads and a bit lower for the latest one.

Table 10: Normlized weights to estimate Figure 4 of the manuscript.

	l=1	l=2	l=3	l=4	l=5	l=6	l=7	l=8	l=9	l=10	l=11	l=12	l=13	l=14	l=15	l=16	l=17	l=18
k=0	100.00%	81.22%	42.00%	29.47%	20.27%	18.90%	15.68%	12.67%	9.79%	8.82%	7.63%	4.91%	3.10%	3.70%	3.29%	2.80%	2.93%	3.62%
k=1		18.78%	47.12%	29.63%	23.50%	16.44%	15.93%	13.69%	11.43%	8.93%	8.15%	7.26%	4.76%	2.99%	3.58%	3.20%	2.72%	2.81%
k=2			10.87%	33.24%	23.62%	19.06%	13.86%	13.91%	12.35%	10.42%	8.25%	7.75%	7.03%	4.58%	2.89%	3.48%	3.11%	2.61%
k=3				7.67%	26.50%	19.16%	16.07%	12.10%	12.55%	11.27%	9.63%	7.84%	7.51%	6.77%	4.43%	2.81%	3.38%	3.00%
k=4					6.11%	21.50%	16.15%	14.03%	10.92%	11.45%	10.41%	9.16%	7.60%	7.23%	6.55%	4.31%	2.73%	3.26%
k=5						4.96%	18.13%	14.11%	12.66%	9.96%	10.58%	9.90%	8.88%	7.32%	7.00%	6.37%	4.18%	2.63%
k=6							4.18%	15.83%	12.73%	11.54%	9.20%	10.06%	9.59%	8.55%	7.08%	6.80%	6.18%	4.04%
k=7								3.65%	14.28%	11.61%	10.66%	8.75%	9.75%	9.24%	8.27%	6.89%	6.60%	5.98%
k=8									3.29%	13.02%	10.72%	10.14%	8.48%	9.39%	8.94%	8.04%	6.69%	6.38%
k=9										2.99%	12.03%	10.20%	9.83%	8.16%	9.08%	8.69%	7.80%	6.44%
k=10											2.74%	11.44%	9.88%	9.47%	7.89%	8.82%	8.44%	7.52%
k=11												2.59%	11.08%	9.52%	9.15%	7.67%	8.56%	8.15%
k=12													2.51%	10.67%	9.21%	8.90%	7.45%	8.26%
k=13														2.40%	10.32%	8.95%	8.64%	7.17%
k=14															2.31%	10.03%	8.69%	8.33%
k=15																2.24%	9.74%	8.35%
k=16																	2.16%	9.39%
k=17																		2.05%
Total	100%	100%	100%	100%	100%	100%	100%	100%	100%	100%	100%	100%	100%	100%	100%	100%	100%	100%

Notes: a) l = number of periods from last treatment change; k = correspoding lead.

17. Appendix A17. Average marginal effect of $Events_{it}$ (estimated via De Chaisemartin and d'Haultfoeuille, 2024) using alternative dependent variables.

Figure 9: Average marginal effect of $Events_{it}$ (estimated via De Chaisemartin and d'Haultfoeuille, 2024).

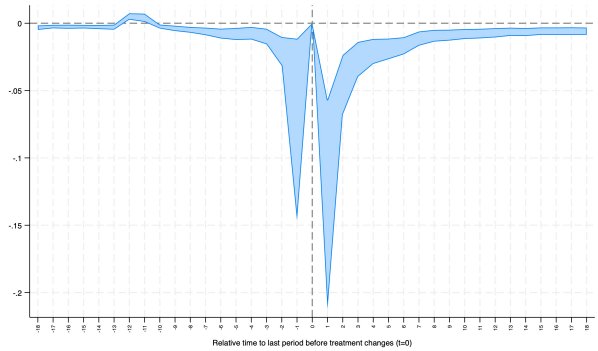

(a) y = $DensLight_{it}$.

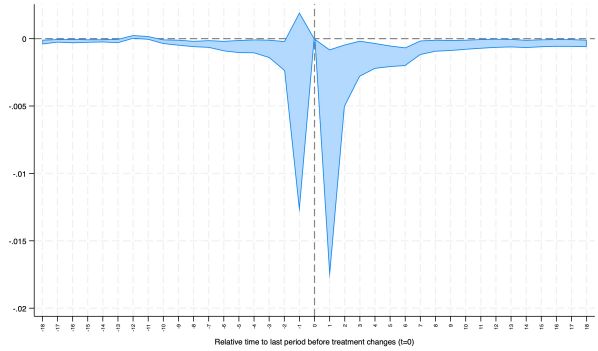

(b) y = $MedLight_{it}$.

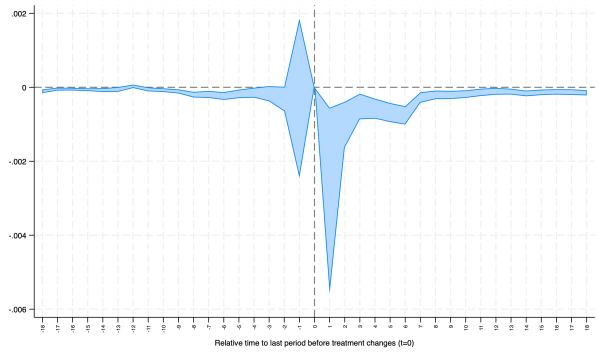

(c) y = $asinh\ MedLight_{it}$.

Notes: a) 95% confidence interval based on clustered robust standard errors at the Raion level is shown; b) the vertical line (dash line on 0) refers to one period (i.e., month) before the treatment change; c) estimated using De Chaisemartin and d'Haultfoeuille (2024) with *normalized weights*.

18. Appendix A18. Within Raion average treatment effect using the estimators of Borusyak et al. (2024) and Callaway and Sant'Anna (2021).

Table 11: Within Raion average treatment effect, *linear* models.

Dependent variable	$IQRLight_{it}$		$p25Light_{it}$		$p75Light_{it}$	
	M1.1 BJS	**M1.2 CS**	**M2.1 BJS**	**M2.2 CS**	**M3.1 BJS**	**M3.2 CS**
$Conflict_{it}$	-0.178***	-0.281***	-0.037*	-0.072**	-0.215***	-0.353***
	(0.055)	(0.079)	(0.019)	(0.035)	(0.072)	(0.109)
Controls *weather-related*	Yes	Yes	Yes	Yes	Yes	Yes
Controls *conflict-related*	Yes	Yes	Yes	Yes	Yes	Yes
Raion FE	Yes	Yes	Yes	Yes	Yes	Yes
Time FE	Yes	Yes	Yes	Yes	Yes	Yes
N	31,144	31,144	31,144	31,144	31,144	31,144

Notes: a) *** p<0.01, ** p<0.05, * p<0.10, b) clustered standard errors at the Raion level in parentheses; c) $IQRLight_{it}$ is the *interquartile range* of the pixel-level distribution within Raion i of night-light at month t; d) $p25Light_{it}$ is the *first quartile* of the pixel-level distribution within Raion i of night-light at month t; e) $p75Light_{it}$ is the *first quartile* of the pixel-level distribution within Raion i of night-light at month t.

Table 12: Within Raion average treatment effect, *asinh-transformed* models.

Dependent variable	*asinh* $IQRLight_{it}$		*asinh* $p25Light_{it}$		*asinh* $p75Light_{it}$	
	M1.1 BJS	**M1.2 CS**	**M2.1 BJS**	**M2.2 CS**	**M3.1 BJS**	**M3.2 CS**
$Conflict_{it}$	-0.077***	-0.114***	-0.020**	-0.034***	-0.074***	-0.110***
	(0.015)	(0.020)	(0.008)	(0.012)	(0.014)	(0.020)
Controls *weather-related*	Yes	Yes	Yes	Yes	Yes	Yes
Controls *conflict-related*	Yes	Yes	Yes	Yes	Yes	Yes
Raion FE	Yes	Yes	Yes	Yes	Yes	Yes
Time FE	Yes	Yes	Yes	Yes	Yes	Yes
N	31,144	31,144	31,144	31,144	31,144	31,144

Notes: a) *** p<0.01, ** p<0.05, * p<0.10, b) clustered standard errors at the Raion level in parentheses; c) $IQRLight_{it}$ is the *interquartile range* of the pixel-level distribution within Raion i of night-light at month t; d) $p25Light_{it}$ is the *first quartile* of the pixel-level distribution within Raion i of night-light at month t; e) $p75Light_{it}$ is the *first quartile* of the pixel-level distribution within Raion i of night-light at month t.

Tables 11 and 12 report the estimates of the within Raion distribution average treatment effect, using the estimators suitable for the staggered design.

Is it still evident the outcome reported in the main manuscript: following the first military event we note that in attacked Raions there is a *shrinkage* of the distribution, with the top part (i.e., the 75th percentile) decreasing more than proportionally than the bottom one (i.e., the 25th percentile). In this sense, we also show that when using such an estimator, the effect on the IQR is larger than those reported by TWFE OLS, hence suggesting that our estimates in the manuscript are rather prudential.

19. Appendix A19. Average treatment effect using spatial controls, with $DensLight_{it}$ as dependent variable.

Table 13: Models with spatial controls. Y = $DensLight_{it}$

	M1	M2	M3	M4	M5	M6
$Conflict_{it}$	-0.707***	-0.304	-0.726***	-0.754***	-0.751***	-0.624***
	(0.237)	(0.226)	(0.206)	(0.251)	(0.237)	(0.191)
asinh mean FC $DensLight_{it}$		5.385***				5.568***
		(1.078)				(1.128)
asinh sum FC $Events_{it}$			0.013			0.208**
			(0.072)			(0.095)
asinh $distZaporizhzhia_i \times PostFebruary2022_t$				-1.389		-0.882
				(1.147)		(1.193)
$BorderRussianControl_i \times PostFebruary2022_t$					2.077***	0.495
					(0.792)	(0.714)
Constant	22482.763***	5566.256	22438.313***	22204.424***	22285.851***	4077.568
	(8318.981)	(5069.890)	(8222.659)	(8127.972)	(8269.415)	(4634.538)
Controls *weather-related*	Yes	Yes	Yes	Yes	Yes	Yes
Controls *conflict-related*	Yes	Yes	Yes	Yes	Yes	Yes
Raion FE	Yes	Yes	Yes	Yes	Yes	Yes
Time FE	Yes	Yes	Yes	Yes	Yes	Yes
N	31,144	31,144	31,144	31,144	31,144	31,144
R2	0.726	0.750	0.726	0.727	0.727	0.751
Within R2	0.044	0.126	0.044	0.044	0.045	0.130

Notes: a) *** p<0.01, ** p<0.05, * p<0.1; b) clustered standard errors at the Raion level in parentheses; c) *FC* = in first contiguous Raions, defined by *Queen Contiguity* logic; d) Controls *weather-related* contains: $Temperature_{it}$ (in linear and quadratic terms), $Rainfalls_{it}$ and $WindSpeed_{it}$; e) Controls *conflict-related* contains: FRP_{it} and $AntiAirDefence_{it}$; f) the model is estimated through OLS TWFE, in Appendix 21 we provide estimates using Borusyak et al. (2024) and Callaway and Sant'Anna (2021).

In Table 13 we provide estimates including the spatial controls when $DensLight_{it}$ in levels is included as dependent variable. As per the model in the main manuscript (employing the *asinh* transformation), in all cases the corresponding average treatment effect associated to $Conflict_{it}$ remains generally negative and statistically significant. In the most complete specification (M6), β is estimated to be -0.624, which is about 10% less than the estimate in Table 5 (M1.3) of the manuscript.

Concerning the specific controls, we find a similar pattern to the one in Table 9 of the manuscript, with a strong evidence of a positive spatial autocorrelation of our dependent variable.

20. Appendix A20. Average treatment effect using spatial controls, with $MedLight_{it}$ and *asinh* $MedLight_{it}$ as dependent variables.

Table 14: Models with spatial controls. Y = $MedLight_{it}$

	M1	M2	M3	M4	M5	M6
$Conflict_{it}$	-0.030*	0.007	-0.031**	-0.034**	-0.032**	-0.021+
	(0.017)	(0.021)	(0.013)	(0.017)	(0.016)	(0.013)
asinh mean FC $DensLight_{it}$		0.489***				0.508***
		(0.124)				(0.131)
asinh sum FC $Events_{it}$			0.001			0.019*
			(0.007)			(0.010)
asinh $distZaporizhzhia_i \times PostFebruary2022_t$				-0.110		-0.082
				(0.098)		(0.076)
$BorderRussianControl_i \times PostFebruary2022_t$					0.109	-0.036
					(0.079)	(0.057)
Constant	1461.201+	-75.137	1459.290+	1439.184+	1450.885+	-209.344
	(932.037)	(535.707)	(914.351)	(914.251)	(925.633)	(471.111)
Controls *weather-related*	Yes	Yes	Yes	Yes	Yes	Yes
Controls *conflict-related*	Yes	Yes	Yes	Yes	Yes	Yes
Raion FE	Yes	Yes	Yes	Yes	Yes	Yes
Time FE	Yes	Yes	Yes	Yes	Yes	Yes
N	31,144	31,144	31,144	31,144	31,144	31,144
R2	0.652	0.677	0.652	0.652	0.652	0.678
Within R2	0.022	0.094	0.022	0.022	0.023	0.097

Notes: a) *** p<0.01, ** p<0.05, * p<0.1; b) clustered standard errors at the Raion level in parentheses; c) FC = in first contiguous Raions, defined by *Queen Contiguity* logic; d) Controls *weather-related* contains: $Temperature_{it}$ (in linear and quadratic terms), $Rainfalls_{it}$ and $WindSpeed_{it}$; e) Controls *conflict-related* contains: FRP_{it} and $AntiAirDefence_{it}$; f) the model is estimated through OLS TWFE, in Appendix 21 we provide estimates using Borusyak et al. (2024) and Callaway and Sant'Anna (2021).

Table 15: Models with spatial controls. Y = *asinh* $MedLight_{it}$

	M1	M2	M3	M4	M5	M6
$Conflict_{it}$	-0.022***	0.001	-0.019***	-0.022***	-0.023***	-0.012**
	(0.006)	(0.006)	(0.005)	(0.006)	(0.006)	(0.005)
asinh mean FC $DensLight_{it}$		0.298***				0.308***
		(0.025)				(0.026)
asinh sum FC $Events_{it}$			-0.002			0.010***
			(0.002)			(0.002)
asinh $distZaporizhzhia_i \times PostFebruary2022_t$				-0.023		-0.022
				(0.033)		(0.033)
$BorderRussianControl_i \times PostFebruary2022_t$					0.038*	-0.042**
					(0.020)	(0.018)
Constant	379.179**	-	386.263***	374.618***	375.540**	-
		557.035***				620.890***
	(147.230)	(92.844)	(145.585)	(143.379)	(146.352)	(89.617)
Controls *weather-related*	Yes	Yes	Yes	Yes	Yes	Yes
Controls *conflict-related*	Yes	Yes	Yes	Yes	Yes	Yes
Raion FE	Yes	Yes	Yes	Yes	Yes	Yes
Time FE	Yes	Yes	Yes	Yes	Yes	Yes
N	31,144	31,144	31,144	31,144	31,144	31,144
R2	0.816	0.875	0.816	0.816	0.816	0.876
Within R2	0.035	0.345	0.035	0.035	0.036	0.353

Notes: a) *** p<0.01, ** p<0.05, * p<0.1; b) clustered standard errors at the Raion level in parentheses; c) FC = in first contiguous Raions, defined by *Queen Contiguity* logic; d) Controls *weather-related* contains: $Temperature_{it}$ (in linear and quadratic terms), $Rainfalls_{it}$ and $WindSpeed_{it}$; e) Controls *conflict-related* contains: FRP_{it} and $AntiAirDefence_{it}$; f) the model is estimated through OLS TWFE, in Appendix 21 we provide estimates using Borusyak et al. (2024) and Callaway and Sant'Anna (2021).

In Tables 14 and 15 we report the estimates using, respectively, $MedLight_{it}$ and its *asinh* transformation as dependent variable.

Again, we find strong evidence on the robustness of our results in presence of such additional spatial controls. It is worth to mention that in Model M6 of Table 14 we find a negative, yet weakly significant estimate of the average treatment effect ($p < 0.12$, indicated by the symbol $+$). In the corresponding estimate using the *asinh* transformation, we find, instead, a negative a significant average treatment effect. As per the other cases, we find that the inclusion of spatial controls tend to lower the estimated average treatment effect, with an estimated which is about half of the one reported in Model M2.3 of Table 1 in Appendix 4.

Finally, we still confirm the presence of strong positive spatial autocorrelation, regardless the definition of the dependent variable, as evidenced in both models M2 and M6.

21. Appendix A21. Average treatment effect using *spatial controls* estimated through Borusyak et al. (2024) and Callaway and Sant'Anna (2021).

Table 16: Models with spatial controls. Estimators for staggered design.

	$\mathbf{y} = DensLight_{it}$		$\mathbf{y} = asinh\ DensLight_{it}$		$\mathbf{y} = MedLight_{it}$		$\mathbf{y} = asinh\ MedLight_{it}$	
	BJS	**CS**	**BJS**	**CS**	**BJS**	**CS**	**BJS**	**CS**
	M1.1	**M1.2**	**M2.1**	**M2.2**	**M3.1**	**M3.2**	**M4.1**	**M4.2**
$Conflict_{it}$	-1.428***	-2.252***	-0.124***	-0.108***	-0.063*	-0.128**	-0.021**	-0.039***
	(0.359)	(0.589)	(0.027)	(0.028)	(0.035)	(0.061)	(0.010)	(0.014)
Spatial Controls	Yes	Yes	Yes	Yes	Yes	Yes	Yes	Yes
Controls *weather-related*	Yes	Yes	Yes	Yes	Yes	Yes	Yes	Yes
Controls *conflict-related*	Yes	Yes	Yes	Yes	Yes	Yes	Yes	Yes
Raion FE	Yes	Yes	Yes	Yes	Yes	Yes	Yes	Yes
Time FE	Yes	Yes	Yes	Yes	Yes	Yes	Yes	Yes
N	31,144	31,144	31,144	31,144	31,144	31,144	31,144	31,144

Notes: a) *** p<0.01, ** p<0.05, * p<0.1; b) clustered standard errors at the Raion level in parentheses; c) *Spatial* Controls include: *asinh mean FC* $DensLight_{it}$, *asinh sum FC* $Events_{it}$, *asinh* $distZaporizhzhia_i \times PostFebruary2022_t$ and $BorderRussianControl_i \times PostFebruary2022_t$; d) Controls *weather-related* contains: $Temperature_{it}$ (in linear and quadratic terms), $Rainfalls_{it}$ and $WindSpeed_{it}$; e) Controls *conflict-related* contains: FRP_{it} and $AntiAirDefence_{it}$.

Table 16 reports the estimate of the average treatment effect, including all spatial controls and using the estimators of Borusyak et al. (2024) and Callaway and Sant'Anna (2021).

In all cases, we find robust evidence of a negative and significant average treatment effect regardless the dependent variable, and whether it is included in levels or *asinh-transformed*. Concerning the *transformed* models, we estimate that in treated Raions, following the first military event, night-light density declined by around -10% (CS) to -11.6% (BJS), while the median by -2.1% (BJS) and -3.8% (CS)[9]. Notably, these estimates, as per all other cases in our manuscript, are larger the canonical TWFE OLS.

[9] All elasticities computed as $e^{\beta} - 1$.

22. Appendix A22. Weighted average treatment effect estimate using TWFE OLS (wOLS), Borusyak et al. (2024) and Callaway and Sant'Anna (2021), all with population weights.

Table 17: Weighted estimates of the average treatment effect.

	wOLS	**wBJS**	**wCS**
$Conflict_{it}$	-0.182***	-0.598***	-0.649***
	(0.042)	(0.112)	(0.135)
Weights	Population	Population	Population
Controls *weather-related*	Yes	Yes	Yes
Controls *conflict-related*	Yes	Yes	Yes
Raion FE	Yes	Yes	Yes
Time FE	Yes	Yes	Yes
N	31,144	31,144	31,144

Notes: a) *** p<0.01. ** p<0.05. * p<0.10. b) clustered standard errors at the Raion level in parentheses; c) w stands for *weighted* model.

Table 17 contains the estimates using canonical TWFE OLS, Borusyak et al. (2024) (i.e., BJS) and Callaway and Sant'Anna (2021) (i.e., CS) with *weights* based on Raions' population.[10]

In all cases, we still maintain a negative and significant estimate of the average treatment effect, yet in this case, the magnitude is rather larger. When using OLS, we find that following the first military event, night-light density decreased by 16% in treated Raions. With Borusyak et al. (2024) and Callaway and Sant'Anna (2021) the estimates raise up to -45% and -47%.[11] This is not surprising, since these estimates reflect the fact that military attacks were concentrated in the most densely populated and likely most economically productive Raions.

[10] The data is retrieved at 2001.

[11] All these estimates are computed as $e^{\beta} - 1$.

23. Appendix A23. Weighted event study plots using TWFE OLS (wOLS), Borusyak et al. (2024) and Callaway and Sant'Anna (2021), all with population weights.

Figure 10: Weighted event study plots. y = $asinh\ DensLight_{it}$.

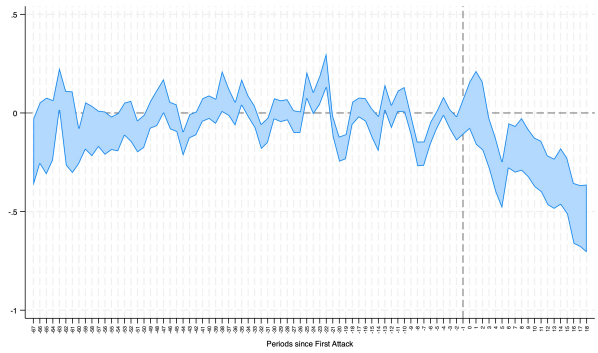

(a) Canonical TWFE OLS estimator.

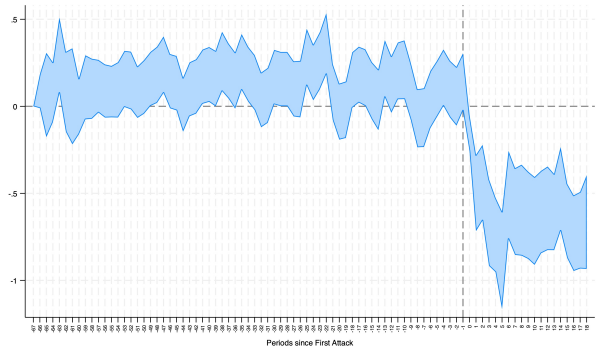

(b) Borusyak et al. estimator.

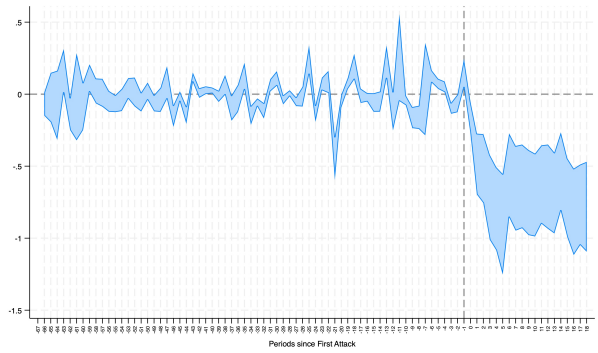

(c) Callaway & Sant'Anna estimator.

Notes: a) 95% confidence interval based on clustered robust standard errors at the Raion level is shown; b) the vertical line (dash line) refers to one month before the treatment (i.e., first military event); c) all models are weighted on Raions' population (in 2001).

References

Borusyak, K., Jaravel, X., and Spiess, J. (2024). Revisiting event-study designs: robust and efficient estimation. *Review of Economic Studies*, 91(6):3253–3285.

Callaway, B. and Sant'Anna, P. H. (2021). Difference-in-differences with multiple time periods. *Journal of Econometrics*, 225(2):200–230.

De Chaisemartin, C. and d'Haultfoeuille, X. (2024). Difference-in-differences estimators of intertemporal treatment effects. *Review of Economics and Statistics*, pages 1–45.

Freyaldenhoven, S., Hansen, C., Pérez, J. P., and Shapiro, J. M. (2021). Visualization, identification, and estimation in the linear panel event-study design. Technical Report n. w29170, National Bureau of Economic Research.

Goodman-Bacon, A. (2021). Difference-in-differences with variation in treatment timing. *Journal of Econometrics*, 225(2):254–277.